STRUCTURE AND EMPLACEMENT OF THE GIANT OKAVANGO DIKE SWARM IN NORTHERN BOTSWANA: A NEW PERSPECTIVE FROM AIRBORNE GEOPHYSICAL DATA

By

ALAN K. LE PERA

Bachelor of Science in Environmental Geology

Rutgers University

Newark, NJ

2012

Submitted to the Faculty of the
Graduate College of the
Oklahoma State University
in partial fulfillment of
the requirements for
the Degree of
MASTER OF SCIENCE
May, 2014

STRUCTURE AND EMPLACEMENT OF THE GIANT OKAVANGO DIKE SWARM IN NORTHERN BOTSWANA: A NEW PERSPECTIVE FROM AIRBORNE GEOPHYSICAL DATA

Thesis Approved:

Estella A. Atekwana

Thesis Adviser

Mohamed G. Abdelsalam

Jack C. Pashin

ACKNOWLEDGEMENTS

This work is supported by the National Science Foundation (NSF) Continental Dynamics grant # EAR 1255233. This is the Oklahoma State University contribution # 2014-013. I thank the Geological Survey of Botswana for allowing free access to their airborne magnetic and gravity data. Additionally, this work could not have been completed without the financial support of the Boone Pickens School of Geology.

I acknowledge Dr. Kevin Mickus, professor at Missouri State University for his guidance with the 3D inversion software and Darren Mortimer, technical product manager at Geosoft In. for providing a full personal license of the Oasis Montaj software package with add-ons used to process and interpret the geophysical datasets. Special thanks to Dr. Colin Reeves of Earthworks for his insightful suggestions and general review of this work.

I thank my committee members Dr. Mohamed Abdelsalam and Dr. Jack Pashin for their knowledge and time, as well as my Advisor Dr. Estella Atekwana for her constant guidance and advice over the past two years. Finally, I thank my peers for their intellectual comments and my family for their constant

support and encouragement throughout my graduate education.

Name: Alan K. Le Pera

Date of Degree: May, 2014

Title of Study: STRUCTURE AND EMPLACEMENT OF THE GIANT OKAVANGO DIKE SWARM IN NORTHERN BOTSWANA: A NEW PERSPECTIVE FROM AIRBORNE GEOPHYSICAL DATA

Major Field: Geology

Abstract: The mode of emplacement of continental dike swarms extending across large distances remains enigmatic and the subject of debate. Here we examine the 1500 km long WNW-trending Okavango Dike Swarm (ODS) in Botswana, Africa suggested as representing a ~180Ma magmatic-tectonic event associated with the initial thermal weakening phase of Gondwana breakup. Historically, the ODS has been interpreted as a failed rift segment of a triple junction based on its geometric relationship with two other prominent dike swarms. Recent studies suggest instead that the ODS was emplaced along a preexisting Precambrian basement lineament. This work examines the lithospheric structural controls on the emplacement of the ODS using gravity and magnetic data. For this we have established the relationship between crustal heterogeneities and the swarm, identified variations in crustal thickness below the ODS, and determined along-strike variations in Curie point depth. Our results show: (1) no apparent basement structures with the same 110° orientation as the ODS, (2) crustal thickness below the swarm ranges from 39-45 km with an average of 42±3 km, indicating the lack of crustal thinning typically associated with rifting, (3) the magnetic basement beneath the swarm extends to a depth of about 24 km and is discontinuous along strike. These high susceptibility axial anomalies conceivably represent fossilized mid-crustal feeder chambers, similar to those found in continental spreading centers such as Afar and Iceland. The lack of significant thinning below the ODS and lack of parallelism with the Precambrian basement fabric suggest the ODS was not associated with a failed rift system and did not actively follow preexisting structures. The ODS is thus interpreted to have been emplaced within the upper crust through magma-enhanced fractures coupled with the presence of a ENE-WSW tensile stress orientation, induced by thermal insulation of the mantle below a stagnant supercontinent and uplift of the asthenosphere..

.

TABLE OF CONTENTS

LIST OF TABLES

Table Page

LIST OF FIGURES

Figure Page

CHAPTER I

INTRODUCTION

Dike swarms can be found in a wide variety of tectonic settings, over a wide range of scales and encompassing a diversity of magma compositions. But on a regional scale, mafic dike swarms are far more common than their felsic counterparts (Rubin, 1995; Ernst et al., 1995). Giant dike swarms represent the remnants of significant tectonic and magmatic events characterized by the highest magma production and effusion rates in the geologic record. Most giant swarms have been implicated in the creation of massive flood basalt provinces and continental breakup, with the orientation and density of dike networks providing an indication of the stresses acting in the crust at the time of their emplacement (Fialko and Rubin, 1999). The term "giant" reflects the unparalleled scale (>300km) of these dike swarms relative to their more modern analogues in active volcanic edifices, sub-volcanic intrusive complexes and rift zones, such as those in Hawaii, Iceland, and Afar. Mechanisms which control the geometry and size of these swarms are highly specialized based on variations in local and regional stress fields, structural framework (faults, folds), lithological arrangement (layering, elasticity) and mode of occurrence among others. For decades it was assumed that these giant swarms formed in response to a mantle plume impinging on the base of the lithosphere (active model).

During the last twenty years however, high resolution data sets and more advanced quantitative methods have begun to challenge long standing assumptions about magma flow dynamics, structural inheritance, and emplacement within giant dike swarms, including the 2500 km Mackenzie swarm in Canada (Ernst and Baragar, 1992) and the 1000 km Gairdner swarm in southern Australia (Parker et al., 1987). The origin and emplacement of the Okavango Dike Swarm (ODS) in northern Botswana has been the subject of controversy, which makes it an ideal laboratory for testing current emplacement models using geophysical techniques.

Historically, the Jurassic ODS has been interpreted as the failed third arm of a conspicuous triple junction in southern Zimbabwe based on its geometric relationship to two other prominent dike swarms (Figure 1) and association with the extensive Karoo Flood Basalt Province (Burke and Dewey, 1972; Reeves, 1978; Cox, 1992). In contrast, it has recently been proposed on the basis of field geological observations that the ODS was emplaced as an inherited polyphase structure, wherein the dikes exploited preexisting basement heterogeneities (Watkeys, 2002; Le Gall et al., 2005; Jourdan et al., 2006). The presence of similarly oriented Proterozoic-age dikes within the central part of the more extensive Jurassic ODS has been used as evidence for the influence of an inherited brittle fabric on emplacement of the younger dikes (LeGall et al., 2002). However, the orientations of both dike sets are not concordant with any mapped basement structures. Thus, it has been insinuated that both dike swarms followed a major Precambrian lithospheric-scale discontinuity that was reactivated during the Mesozoic (Jourdan et al., 2004; Le Gall et al., 2005).

The interpretation and characterization of the ODS has historically involved a comprehensive collaboration of different research methods including: (1) in-situ field measurements, (2) high-precision age dating methods, (3) aeromagnetic and gravity coverage and (4) paleomagnetic and geochemical studies, which have provided insights into its age, shape, orientation, and geochemistry (Duncan et al., 1997; Reeves, 2000; Jourdan et al., 2004; Auborg et al, 2008).

However relative to the lateral extent of the ODS, most investigations were restricted to local outcropped areas, which have provided insights into the swarms age and chemistry, but are inadequate for explaining regional emplacement of the swarm. Outside of the Shashe River area (Figure 2a), where the dikes are exposed, little is known about the geometric character of the swarm and its relationship to the lithospheric structure. This lack of knowledge stems primarily from limited seismic or magnetotelluric (MT) survey coverage (Fouch et.al, 2004; Miensopust et.al, 2011) and sparsely distributed borehole data.

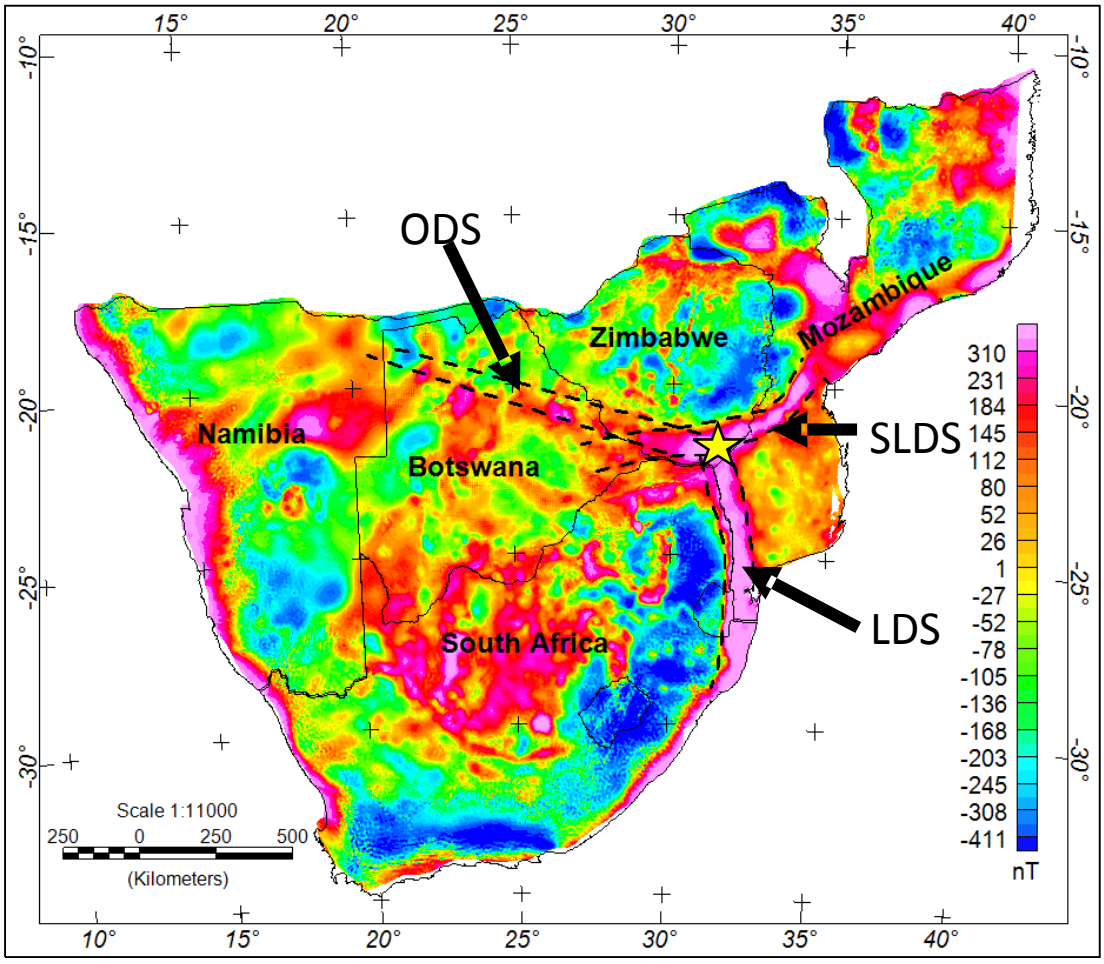

Figure 1: Bouguer anomaly map (1.25 km spatial resolution) of southern Africa showing the location of the three primary dike swarms converging near Mwenezi (yellow star) forming a conspicuous rift-rift-rift triple junction. Dashed lines indicate general extents of the different swarms: ODS = Okavango Dike Swarm, SLDS = Save-Limpopo Dike Swarm, LDS = Lebombo Dike Swarm.

A peculiar characteristic of the ODS is its oblique orientation in relation to preexisting structures in the Proterozoic basement of southern Africa. A detailed analysis of the entire ODS is important for understanding the regional expression of continental dike swarms and can be used to demonstrate the usefulness of geophysical methods for mapping swarms in areas where they are concealed in the subsurface. With the exception of a small trend rotation from 110° to ~106° near the Limpopo orogenic belt (Figure 2a), the ODS remained almost perfectly linear as it propagated toward the north-west, where it cross-cuts a complex arrangement of Achaean cratons, Proterozoic orogenic belts, a shear zone, and Permo-Jurassic sedimentary and volcanic rocks (Figure 2a and b). Structural and statistical analyses of Precambrian terranes indicate that the preferred strike in northern Botswana is NNE-SSW (Figure 3; Modie, 1996; Johnson et al., 1996; Key and Ayres, 2000; Bordy, 2010). The ODS, on the other hand, has a mean strike of WNW-ESE, indicating that the emplacement of the dikes was not affected by the orientation of these pre-existing terranes.

Available high-resolution potential field data collected over the last two decades has provided an opportunity to undertake a detailed regional analysis of the ODS. The purpose of this work is to integrate aeromagnetic data with gravity and previous studies across the length of the ODS to map the geometric characteristics of the swarm and investigate swarm emplacement in relation to the regional geologic framework and proposed emplacement models. Specific objectives include: (1) determining the role of crustal heterogeneities on emplacement of the ODS, (2) identifying variations in crustal thickness below the ODS, as compared with incipient and paleo-rift systems, (3) determining along-strike variations in Curie Point Depth (CPD) below the swarm, to determine if there is or ever was a thermal perturbation within the lithosphere, that might reveal the role of asthenospheric processes during emplacement, and (4) suggesting a model for dike emplacement along an approximately 1500 km linear path.

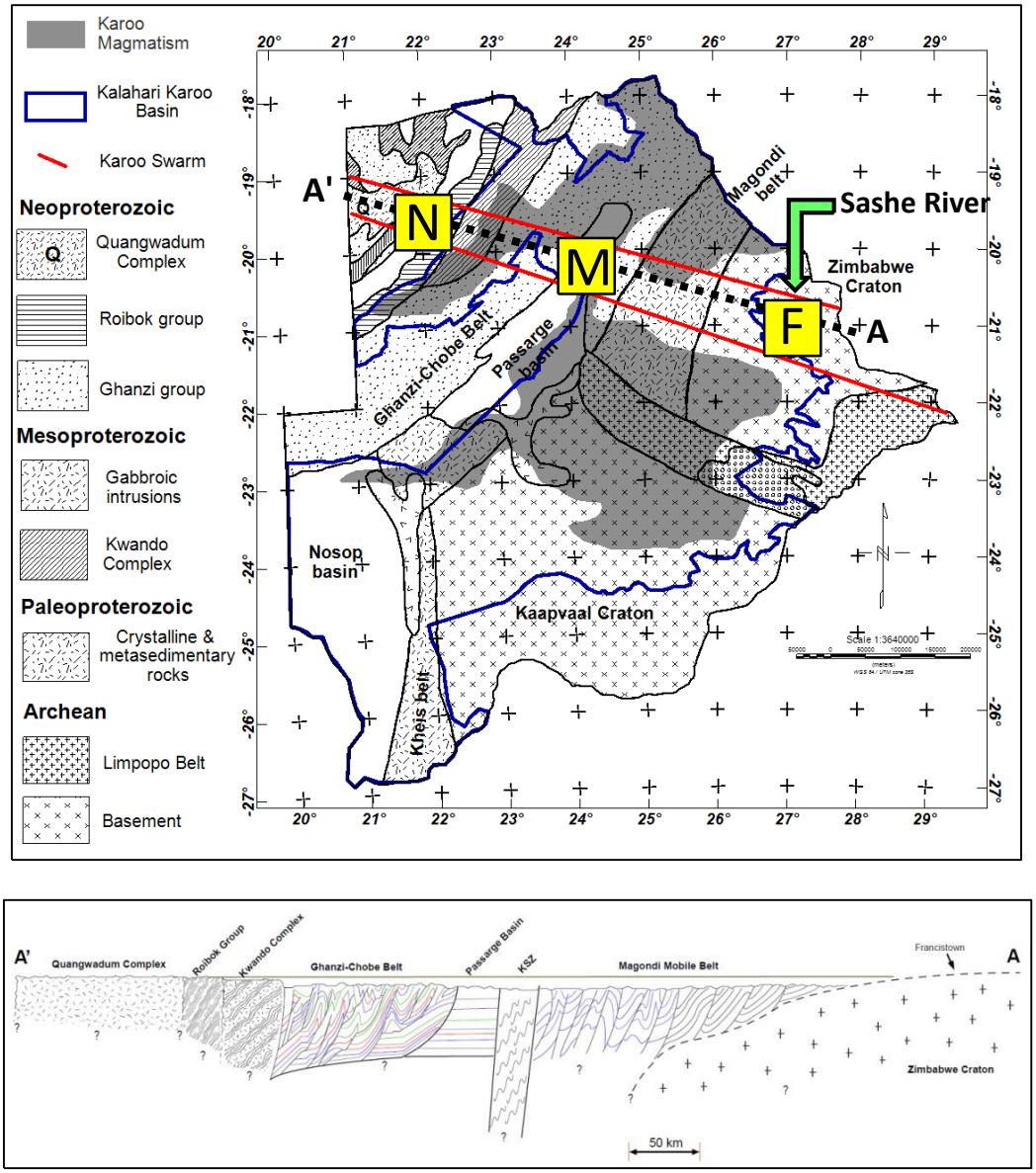

Figure 2: (Top) Subsurface Precambrian geology map of Botswana created from a compilation of Jones (1980), Singletary (2003), Jourdan et al. (2007), and Bordy et al. (2010). Black lines represent approximate boundaries between geologic terranes. Blue lines show the interpreted extent of the Kalahari Basin and Karoo Flood Basalts. Red lines outline the general trend and extent of the ODS across Precambrian terranes and structures. (Bottom) hypothetical cross section along profile A-A' (dashed black line in figure 2a) depicting the structural complexity of northern Botswana. Cross-section was created based on literature review and geophysically defined terrane boundaries (Jones, 1980; Johnson et al., 1996; Modie, 1996; Majaule et al., 2001; Key and Ayres, 2000. The relative degree of thrusting, folding, and shearing was drawn based on available structural information from Zimbabwe (Treloar, 1988). Yellow rectangles showing: F-Francistown, M-Maun, N-Ngami areas.

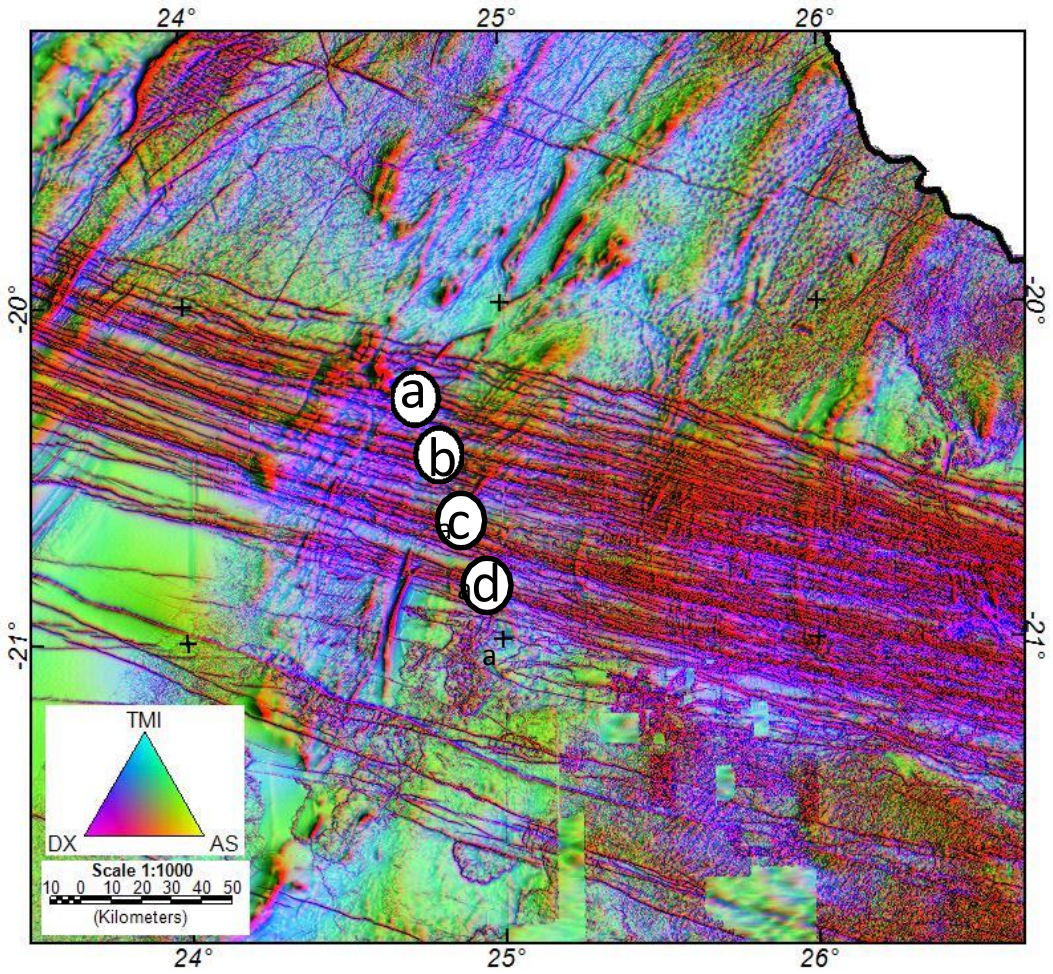

Figure 3: Ternary map of northern Botswana depicting the dominant NNE-SSE orientation of the pre-existing geologic basement terranes and ESE trending ODS. Three filters used are: 1st order vertical derivative (DZ) - pink/red, total magnetic intensity (TMI) - blue/green and analytic signal (AS) – yellow/orange. Letters a-d, represent four main dike clusters developed during emplacement of the swarm as regionally depicted in Figure 6.

CHAPTER II

REVIEW OF LITERATURE

2.1 Tectonic setting

The ODS is part of the Mesozoic Karoo Large Igneous Province (LIP) in southern Africa, whose formation has been correlated broadly with the early stages of Gondwana breakup, although details of the temporal relationship remain unclear (Duncan et al., 1997). The ODS is one of three major dike sets in southern Africa (Figure 1), including the N70°E trending Save-Limpopo Dike Swarm (SLDS) and N-S trending Lebombo Dike Swarm (LDS). The three dike sets appear to radiate out from the Mwenezi (formerly Nuanetsi) region in southern Zimbabwe, proposed to be the central magma source for the dikes (Burke and Dewey, 1972; Cox, 1992; Duncan et al., 1997; Reeves, 2000). The pattern and orientation of the three dike sets led to the suggestion that they were formed in association with the development of a rifted triple junction. However, detailed geochronological and structural data of the different dike sets forming the conspicuous triple junction-like pattern lack in their ability to firmly establish synchronous and cogenetic emplacement as would be expected from a mantle plume model (Le Gall et al., 2005). Although the Okavango and Save-Limpopo dike swarms (SLDS) have been determined to be the same age, they do not actually radiated out from the same location, but rather crosscut and partially overlap one another in the Tuli Basin area near the eastern boundary of Botswana. The northern Lebombo dike swarm (LDS) is comprised of several generations of feeder dikes directly

correlated with numerous volcanic units, but has been dated 1-2 Ma older than the ODS and SLDS.

It has been suggested that the ODS was emplaced during the initial weakening phase of Gondwana. Although crustal fragmentation did not start until the Late Jurassic-Early Cretaceous, the stresses and magmatism responsible for the final breakup had been developing since the Permo-carboniferous (≈300 Ma; Guirand and Bellion, 1995). The most common model for anorogenic magmatism is the impingement of an active plume head on the base of the lithosphere (Burke and Dewey, 1972; White and McKenzie, 1989; Campell and Griffiths, 1990). However, based on geochemical and structural data, it was concluded that the ODS was not sourced by a mantle plume (Jourdan et al., 2004; Le Gall et al., 2005). Morgan (1981) positioned the Bouvet hotspot in the vicinity of the southern Zimbabwe triple junction at 200 Ma. According to Courtillot et al. (2003), the Bouvet and 20 other hotspots in the Pacific and Indo-Atlantic hemispheres existed as upper mantle features linked to the asthenosphere, passively responding to lithospheric fracturing. His interpretation follows the "top down" plate tectonic model proposed by Anderson et al. (1982; 1994; 2001; 2002) and Hamilton (2003), in which the temporary stagnation of a supercontinent causes thermal insulation of the mantle, leading to the expansion and bulging of the asthenosphere.

Thermal expansion of the mantle would lift the supercontinent, placing it under tensional stress as it adjusted to the increased radius of curvature, causing the internal zones of weakness (suture zones) to reactive and begin fracturing from the upper lithosphere downward. Plate tectonic processes later exploited the initial fractures that were able to extend down to a magma source, there after becoming conduits of flow towards the surface, resulting in large igneous outbreaks and hot spots, widen rifts, and dispersion of rifted segments. As a follow up, Sears et al. (2001; 2004) looked at the relationships between known hot spots, LIPs, and configuration of the continents during the Mesozoic. They proposed that the lithosphere would fracture along a geometrically defined pattern composed of quasi-hexagonal tessellation vertices under the

conditions of isometric, uniaxial tension, such as when a continental scale asthenospheric bulge is pressing on the base of the lithosphere (Figure 4). This truncated icosahedron pattern is based on Euler's formula for arbitrary polyhedrons on a spherical surface, which has been demonstrated in columnar joint and mud crack studies to relieve the greatest amount of strain energy for the least amount of work invested in the nucleation and propagation of fractures (Jagla and Rojo 2002).

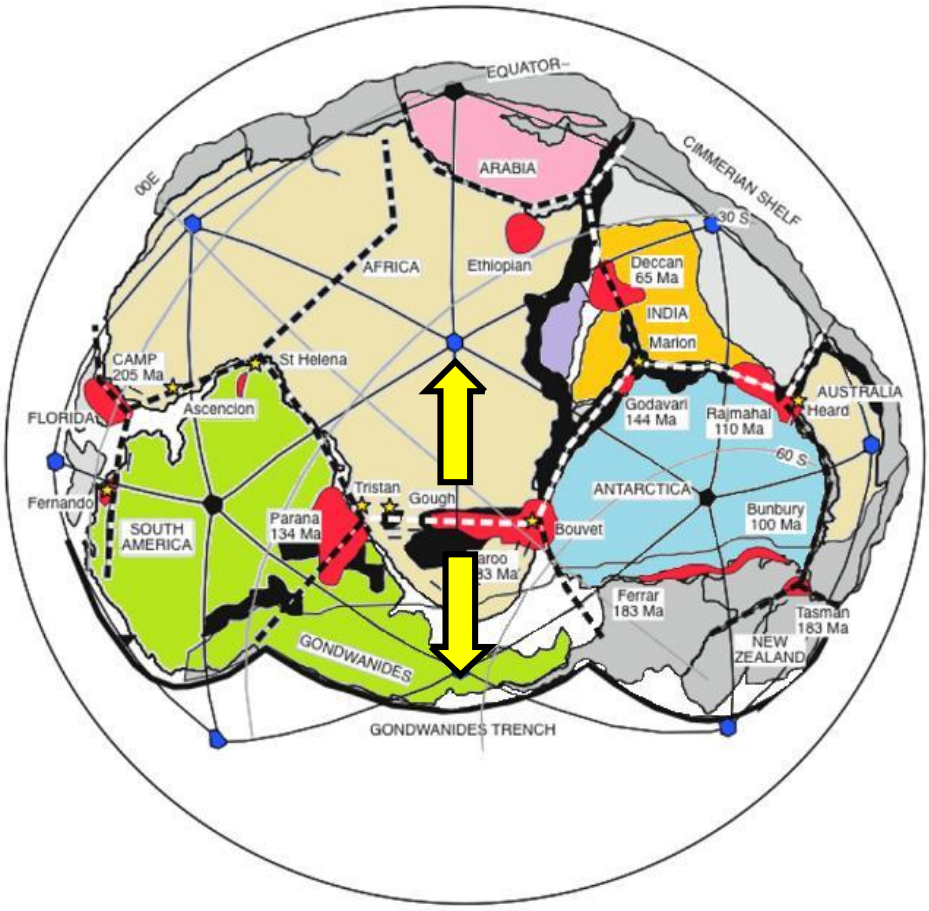

Figure 4: Gondwana tensile stress tessellation modified from Sears et al. (2004). The icosahedral stress tessellation (thin solid lines) is displayed overlying the fracture tessellation (heavy dashed lines) such that vertices of the stress tessellation occupy faces of the fracture tessellation, and vice-versa. Gondwana fragmented along these radial fractures, guided by the tensile stress distribution. This fracture arrangement provided the most strain relief for the least amount of work. Red areas indicate prominent large igneous provinces, including the Karoo in southern Africa. Black areas indicate the locations of Permian basins. Yellow arrows indicate the proposed direction of tensile stress during the emplacement of the ODS.

2.2 Okavango Dike Swarm

2.2 Okavango Dike Swarm

Aeromagnetic studies of Botswana show that the N110°E trending ODS extends for ~1500 km (720 km in Botswana) from Southern Zimbabwe to Namibia, with a gradual westerly narrowing of the high-density dike zone from about 100 km near Francistown to about 50 km in the Maun area (Reeves, 1978, 2000; Gomez, 2001). Proterozoic and Jurassic aged dikes are virtually indistinguishable using aeromagnetic data due to their nearly identical petrographic features. Based on our current state of knowledge, there is no distinct relationship between the age of a dike swarm and its relative size other than the fact that most major swarms developed during large scale tectonic periods with no modern analogues (Ernst et al., 1995). Geochronological data taken from dike samples collected near Francistown (Figure 2a) yielded concordant $^{40}Ar/^{39}Ar$ plateau ages from 178.4± 1.1 to 180.3± 1.3 Ma, suggesting that the ODS was emplaced during the early Jurassic as either one short-lived igneous event or a succession of smaller magma injections (Elburg and Goldberg, 2000; Le Gall et al., 2002). Other studies have shown that the ODS cross-cuts thick layers of flood basalts indicating that it must post-date the main Karoo magmatic event. In addition, the Proterozoic dikes were determined to have been emplaced between 851± 6 to 1672± 7 Ma (Jourdan et al., 2004).

Rapid quantitative analysis of exposed dikes along the Shashe river in NE Botswana (Figure 2a) indicated that the length of individual dikes ranges from 1-18 km and the mean width of individual dikes ranges from 15-20 m (Le Gall et al., 2002). Based on the anisotropy of magnetic susceptibility, Aubourg et al. (2008) determined that the ODS was fed vertically within 300 km of the triple junction area, but transitioned into dominantly lateral flow after 400 km away from the source area. These results are consistent with Ernst and Duncan, 1995, who were the first to propose lateral flow to the west in the ODS. For the most part, the top of the ODS is buried beneath Kalahari sands with an average depth of ~50 m and a maximum depth of ~250 m within the Okavango rift zone due to displacement of the bordering normal faults.

CHAPTER III

METHODOLOGY

3.1 Imaging near-surface structural trends

High-resolution aeromagnetic data were used to map crustal blocks and structural trends crosscut by the ODS. The magnetic data used in this study were acquired in 1996, with a line spacing of 250 m and at an altitude of ~80 m. Variations in regional swarm arrangement were mapped using filters, such as reduction to pole (RTP), analytical signal, 1st order derivatives, tilt derivative and upward continuation. Additionally, a number of ternary maps were generated from a combination of these filters, in order to enhance the shallow magnetic signature of the dikes.

3.2 Imaging the magnetic base of the Okavango Dike Swarm

The depth and geometry of the base of the ODS was evaluated using 3D inversions of the residual aeromagnetic anomaly data to estimate the CPD with the assumptions that: (1) the dikes were emplaced laterally (from ESE to WNW), away from their source region near Mwenezi and (2) they persisted in the upper crust above the curie isotherm. The CPD is the temperature at which spontaneous magnetization is lost and magnetic minerals become paramagnetic. Rocks typically lose their magnetism at temperatures greater than the Curie isothermal point of magnetite (~580 ºC) at atmospheric pressure. The depth of the base of the magnetized crust is directly related to CPD, and the variation in this depth reflects variation in the temperature of the

crust (Hussein et al., 2012). Inversion models were generated using the *MAG3D* modeling software developed by the University of British Columbia, based on the algorithm of Li and Oldenburg (1996).

Computation time was reduced by subdividing the 720 km long dike swarm into eleven ~1° x 1° squares (Figure 5), each of which was re-sampled to a grid size 1500 m from the original 65 m and was separately processed using the same input parameters. Individual inversions were merged to produce and overall picture of how magnetization varied along-strike of the swarm. In order to reduce the edge effect, the squares were overlapped by 40% on each side, with the exception of the two end squares. An apparent susceptibility range of 0.0-0.04 SI was used for the inversions, creating a contrast of 0.033 SI between the dike related magnetic anomalies and the background geology. It is important to note that the CPD values determined from the inversion process are not necessarily the lower limit of a geologic feature being imaged, but rather the depth below which the material is no longer magnetic.

In general, the area analyzed to determine the depth to the base of a magnetic anomaly must be at least three to four times the expected depth to the source (Bouligand et al., 2009). In order to ensure that the response of the deepest layers were captured in this analysis, a few specific 200 km x 200km and 400 km x 400 km windows were also used and the depth weighting procedure of Hussein et al., 2012 was utilized to circumvent the problem of near surface magnetic anomalies. To obtain reliable results in lack of external constraints from heat flow models or borehole information, different inversion parameters such as data errors, starting models and mesh size were constantly adjusted so that the inversion model best reflected the geology of the area (Hussein et al., 2013; Maden, 2010). The final grid mesh was set at 900 km², with a constant topography of 80 m (flight height) and an acceptable range of error equal to or less than 2%. The maximum depth of the squares was set at 50 km, and the magnetic susceptibility range used was based on the magnetic anisotropy results of Aubourg et al. (2008), specifically 0.0 – 0.04 SI respectively.

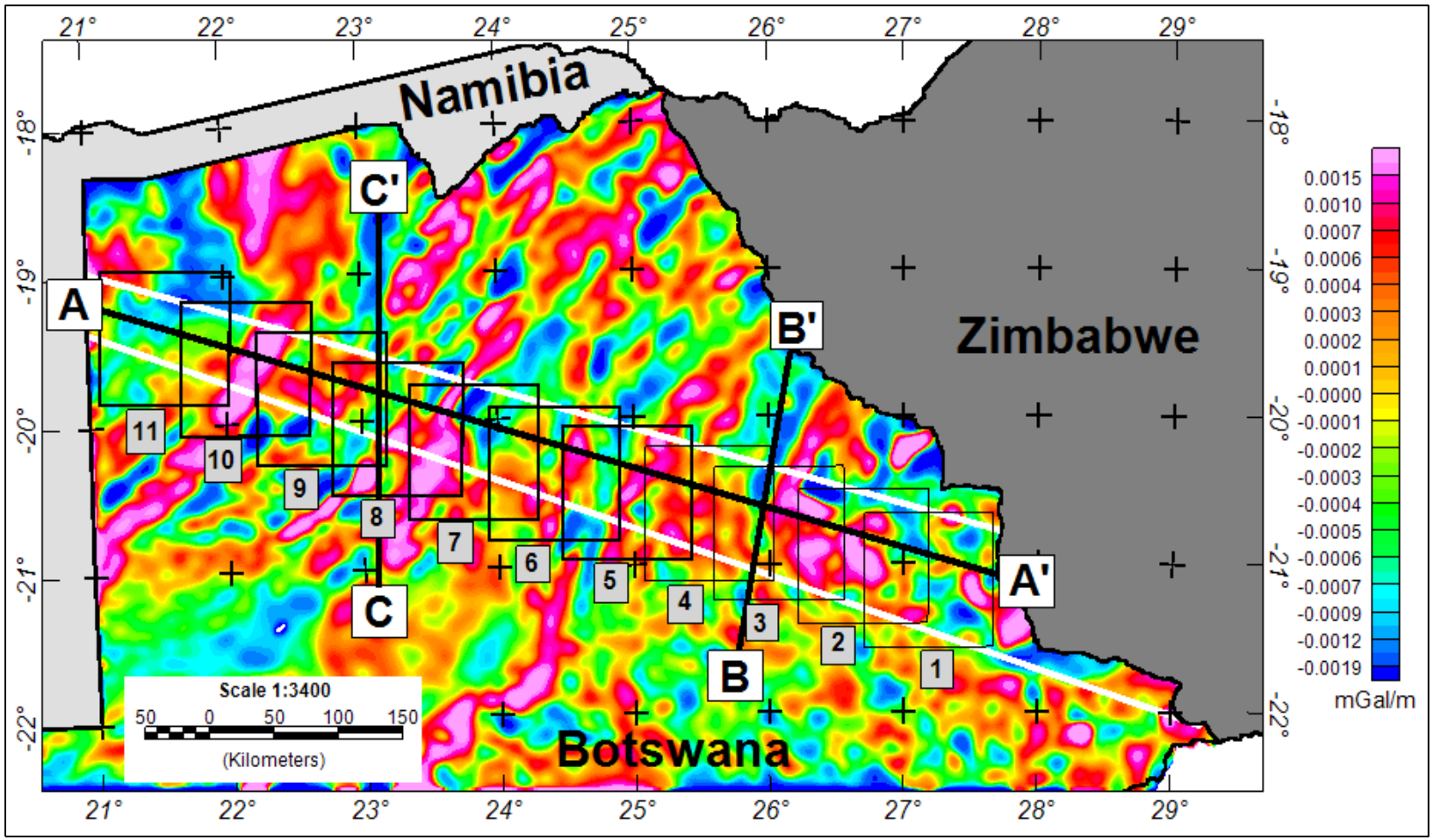

Figure 5: 1st vertical derivative Bouguer anomaly map of northern Botswana depicting large along-strike discontinuous gravity highs associated with Achaean greenstone belts and Proterozoic basement structures. The lack of a consistent gravity high along the length of the ODS, attributable to crustal thinning and lack of a narrow gravity low along the same strike, characteristic of thick sedimentary rift basins, suggest that the swarm did not form in association with a failed rift system. Eleven inversion blocks with 40% overlap are superimposed onto the gravity map. Lines A-A', B-B' and C-C' show the location of the lithospheric cross sections in Figures 9-10.

3.3 Imaging the crustal thickness beneath the Okavango Dike Swarm

Crustal depth values (Moho depth) across northern Botswana were estimated using the 2D radial average power spectrum method. The method of depth estimation through spectral analysis has been widely used by several authors for both magnetic and gravity data (Tselentis et al., 1988; Maus and Dimri, 1996; Maden, 2010; Hussein et al., 2013). We utilized a composite gravity data set assimilated from a 7.5 km survey performed by the Geologic Survey of Botswana, supplemented by additional data sets acquired from various industry sources, and a higher resolution (2 km) data set collected as part of the National Science Foundation (NSF) funded PRIDE (Project for Rift Initiation Development and Evolution) project (Figure 5). The radial average power spectrum method is based on an observation by Spector and Grant (1970) that the depth factor invariably dominates the shape of a 2D power spectrum curve. The radially averaged power spectrum of potential field data within a 2D observation plane decreases with increasing depth by a factor of ($-2hr$), where h is the depth to the top of the source and r is the wavenumber. Hence, the depth to source can be derived directly from the slope of the log radially averaged power spectrum curve.

Breaks in the slope of the power spectrum curve represent density discontinuities (Gomez-Ortiz et al., 2005). As an example, Figure 6 shows the spectrum curve for one of our Bouguer anomaly windows (not shown). Three frequency domains are defined in this figure. The first one, domain A, corresponds to a frequency of up to 0.08 km^{-1} and the mean depth of the source as determined from the slope of the linear segment fitted to the data is 88.7 ± 2 km. The second one, domain B, corresponds to a frequency ranging from 0.08 to 0.32 km^{-1} and the mean depth of the source is 19.6 ± 2 km. The third domain comprises the final part of the power spectrum and is considered based on its mean depth (<5 km^{-1}) to be noise.

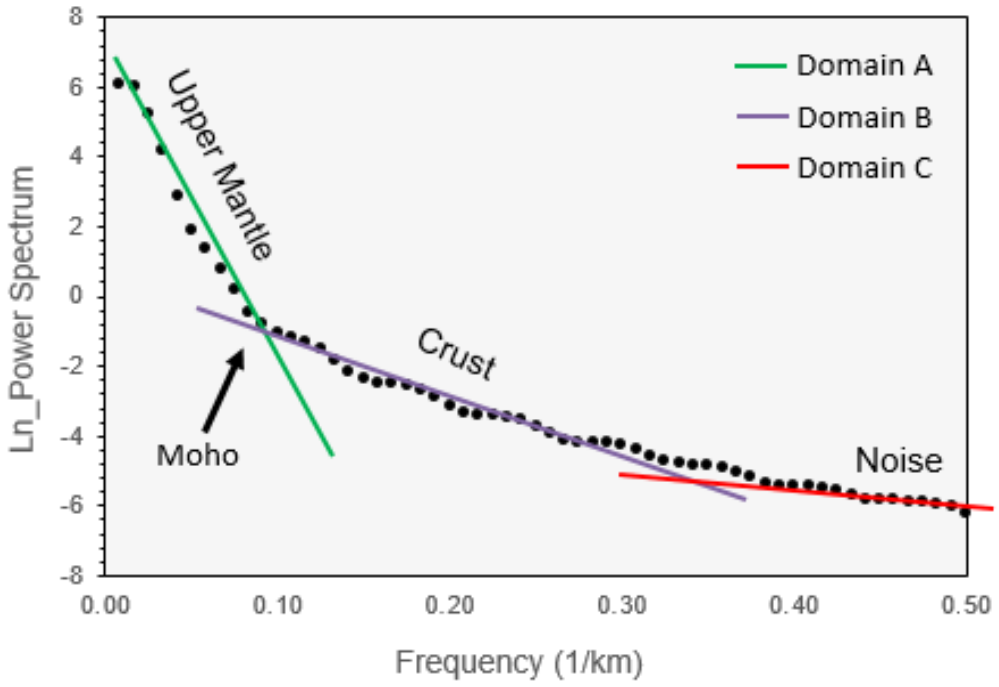

Figure 6: Graph representing the natural logarithm of the radial gravity power spectrum versus the frequency for the Bouguer anomaly window. Three domains are recognized: the upper mantle (A), the crust (B) and noise (C). The Moho discontinuity represents the boundary between the crust and mantle.

To calibrate our Moho depth estimations, we calculated the crustal thickness of eight blocks correlating with the locations of eight passive seismic stations from previous studies following the Southern African Seismic Experiment (SASE) (Table 1; Nair et al., 2006; Kgaswane et al., 2009; Youssoff et al., 2013). The frequency range of 0.06 to 0.13 km^{-1} used for Moho depth estimations toward the NW (where seismic values were unavailable) was determined as the mean of these eight stations. Crustal thickness was estimated as the average of the maximum and minimum gradient of the second break in slope within the calibrate frequency range. Spatial resolution was improved through subsequent window size adjustment, being careful not to remove or alter the spectral peak.

Table 1. Crustal thickness estimation from gravity compared to data from passive seismic stations in eastern Botswana from the Southern African seismic experiment (SASE).

Seismic Station	Longitude (deg)	Latitude (deg)	Nair et al., 2006 (km)	Kgaswane et al., 2009 (km)	Youssoff et al., 2013 (km)	Lepera et al., 2014 (km)
Sa63	27.20	-22.84	42.3± 0.26	N/A	43.0	41.3± 1
Sa54	26.25	-22.81	N/A	40.5	N/A	46.7± 1
Sa65	27.22	-22.82	43.1 ±0.33	40.5	43.0	43.5± 1
Sa66	26.37	-21.90	46.9 ±0.16	48.0	46.5	46.3± 1
Sa67	27.20	-21.92	N/A	45.5	39.5	47.1± 1
Sa68	28.19	-21.95	50.3 ±1.19	45.5	41.0	51.0± 1
Sa70	26.36	-21.09	51.6 ±0.23	50.5	50.5	52.6± 1
Sa71	27.14	-20.93	43.6 ±0.85	43.0	40.5	42.9± 1

CHAPTER IV

FINDINGS

4.1 Relationship between the Okavango Dike Swarm and pre-existing structures

From ESE to WNW, the ODS crosses the Zimbabwe craton, the Magondi orogenic belt, the Kalahari suture zone, the Passarge basin, the Ghanzi-Chobe orogenic belt, and the Kwando complex (Figure 7). NE-trending fold axial surfaces were mapped from the aeromagnetic data within most of these Precambrian terranes with the exception of the Passarge basin (Figure 7). Additionally, numerous fractures up to 60 km long were mapped at the northern extent of the Kalahari suture zone and the Ghanzi-Chobe orogenic belt (Figure 7). The fractures are interpreted to have been created during the Neoproterozoic Pan African orogeny, when the Kalahari suture zone was developed as a major shear zone. Many of these structural features are not directly cutting the ODS, but represent the predominant orientation of the basement, through which the dikes were emplaced. Apart from the dikes themselves, there are no apparent basement heterogeneities striking N110°E in the areas toward the NW where dike prevalence is not overbearing (Figures 3 and 7). Despite along strike rheological variability and significant Precambrian deformation, the dikes themselves shows little deviation in their path as they transition from one geologic terrane to the next.

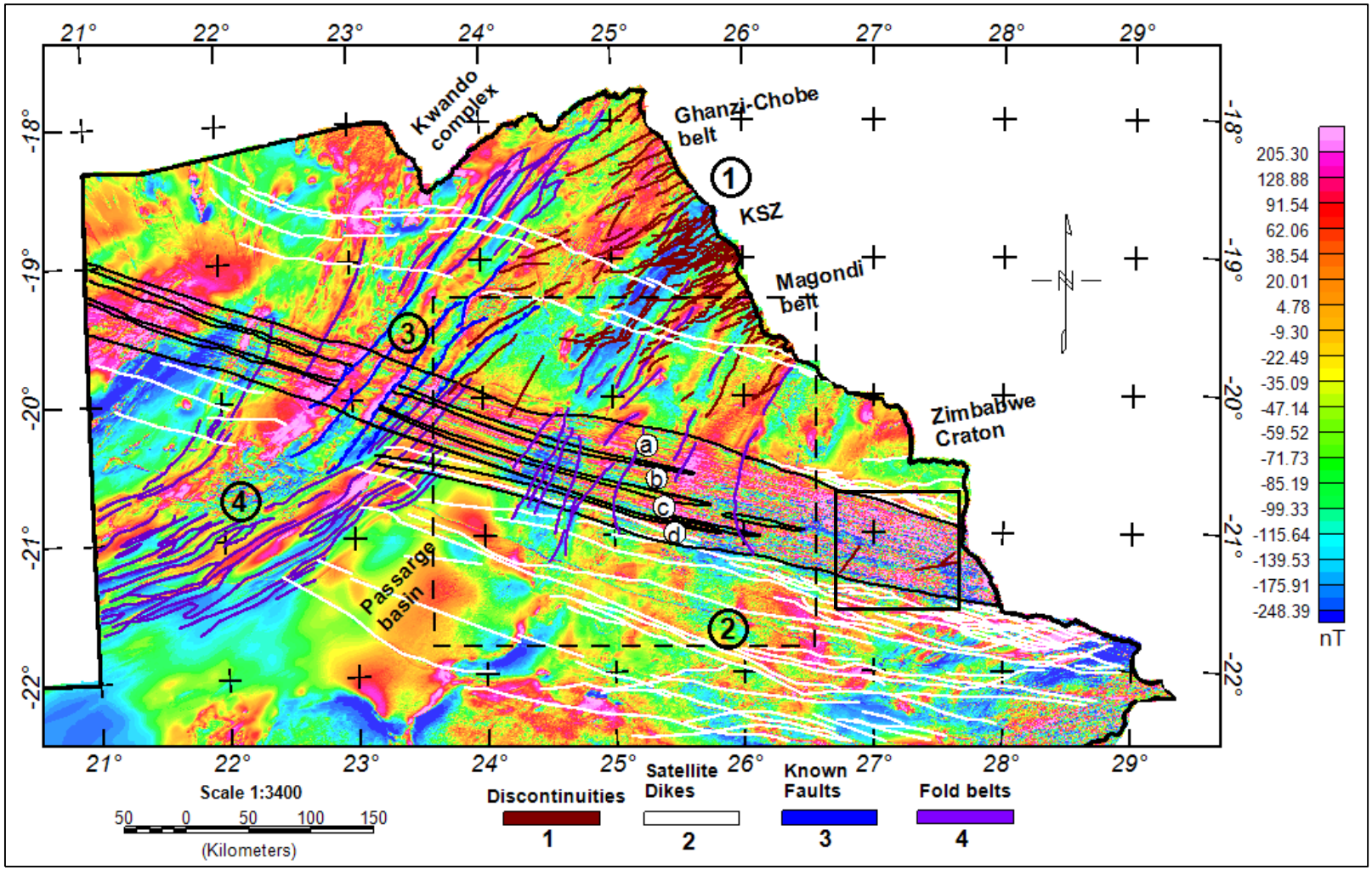

Figure 7: Detailed structural interpretation of northern Botswana and along-strike segmentation of the ODS, superimposed on a total magnetic intensity grid. Interpretations were based on a compilation of grid filters such as analytic signal, tilt, first/second order derivatives and ternary maps. The high-density (primary) section of the dike swarm was divided into four main channels (a-d), separated from one another by areas of minimal or absent dikes. Black solid box indicates location on inversion block one, shown in detail in Figure 8. Black dashed box indications location of detailed ternary map, shown in Figure 3.

During the transition from the Zimbabwe craton into the Magondi orogenic belt, the ODS breaks into four clusters separated from one another by areas of minimal or absent dikes. The three northern clusters (labeled a-c in figure 7) traverse the entire 720 km distance across northern Botswana while the southern cluster (labeled d in Figure 7) deviates from the N110°E orientation and terminates within the Ghanzi-Chobe belt. The width of individual clusters decreases from 16-26 km near the Magondi orogenic belt to less than 12 km near the Kwando complex (Figure 7). Consequently, the width of the swarm as a whole changes from 75 km near Francistown to less than 50 km near Maun (Figure 2). Although clusters "c" and "d" are depicted as being about the same width in the NW as they are in the central part of the swarm, the apparent width results because the number of dikes exposed is smaller but the distance between them is larger. Furthermore, preexisting structures and dikes that juxtapose the ODS may be unrecognized near Francistown due to a high dike density.

4.2 Crustal magnetic structure of the Okavango Dike Swarm

As discussed earlier, the magnetic base of the ODS was imaged using 3D inversions of eleven blocks dividing the entire length of the swarms (Figure 5). Variations in the depth to the base of the magnetized crust are directly related to the CPD, beyond which spontaneous magnetization is lost and magnetic minerals become paramagnetic. Figure 8 is a detailed view of inversion block one, shown in Figure 7. Five vertical across strike slices taken from this block show that the subsurface expression of the ODS is an ~80 km wide U- or V-shaped anomaly, with the deepest part of the anomaly existing near the center. The base of the anomaly extends to a maximum depth of ~24 km, but shallows to less than 12 km in the north and south. This pattern of a deeper anomaly fanning upward into shallower depths is consistent in all inversion blocks along strike of the ODS. However, the location and size of these deeper source points is not always central to the near surface expression of the dikes. Consequently, the shape of the anomaly is not always symmetrical. The basic architecture of the feeder dikes is very well

depicted in vertical slice "b" in Figure 8. They branch upwards from the central source, starting at first as wide pipes, which later diverge into smaller stems.

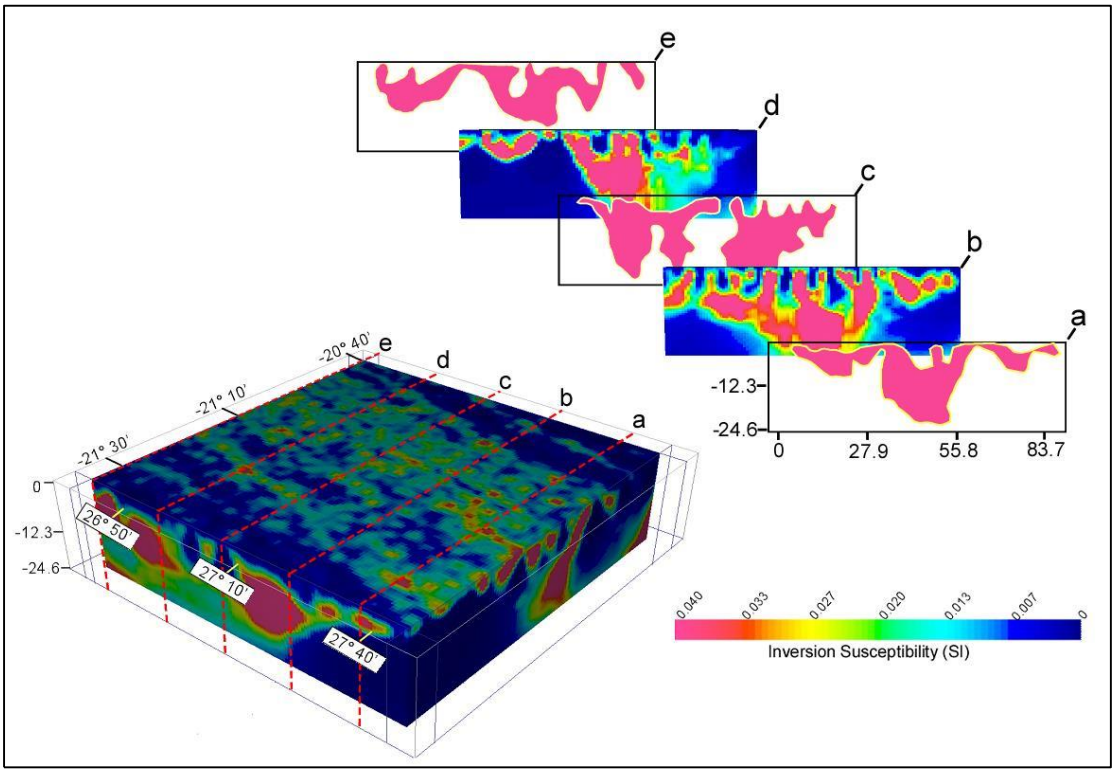

Figure 8: 3D inversion of a 100 km x 100 km aeromagnetic block (Block 1; Figure 5) covering part of the ODS, with five vertical across-strike slices showing a more detailed look at the ~80 km wide U- or V-shaped subsurface expression of the swarm. The 3D inversion results suggest that the ODS' basic sub-surface architecture include shallower feeder dikes being fed from deeper, centrally located source, possibly magma chambers. The block is entirely ecompassed within the interpreted boundaries of the Zimbabwe Craton. The magnetic basement extends to a maximum depth of ~24 km, but varies slightly along-strike. Susceptibility contrast between the dikes and the granitic-gneissic background reaches 0.033 SI. See Figure 5 for the location of the aeromagnetic block.

To further illustrate the crustal structure in northern Botswana, one along strike and two across strike sections of the ODS were developed. The locations of the three profiles are shown in Figure 5. Along strike profile A-A' (Figure 9) shows a maximum CPD of 25 km near the WNW and ESE extents of the swarm in areas closely associated with the interpreted outer limits of the Zimbabwe Craton and Congo Craton. The average depth of the CPD is less than 23 km below the Precambrian orogenic belts and suture zones. Depth to the base of the magnetic anomaly produced by the ODS is discontinuous between the Magondi orogenic belt and Roibok complex

(Figure 9), varying from 23 km at the edges of major terrane boundaries to less than 10 km within the Okavango rift zone and in areas interpreted herein to be the locations of shallow, laterally propagating dikes. Although the dikes can be traced across Botswana into Namibia, they are not well represented in the inversions beyond the Kwando complex because their signatures are obscured by the background geology, as less of them were able to reach this distance.

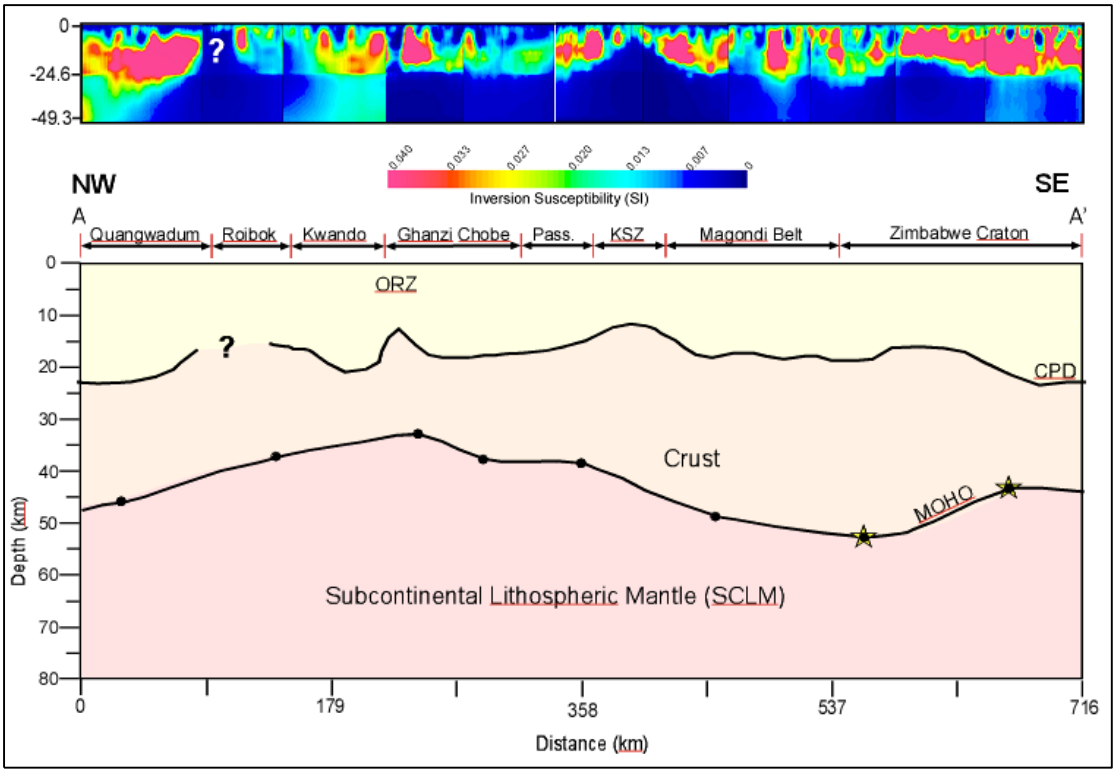

Figure 9: A schematic NW-SE lithospheric section (A-A' in Figure 5) illustrating the along-strike variation of CPD and crustal thickness below the ODS. Deep magnetic anomalies are potential along-strike magma chambers, whose size and shape was controlled in part by Precambrian heterogeneities.

In profile B-B' (Figure 10), the deep CPD is confined to the area directly below the ODS and retains the same U-shaped channel shown in Figure 8. The 3D inversion shows that the CPD directly below the swarm extends to a maximum depth of ~24 km, but rapidly decreases to less than 10 km at the edges of the ODS, beyond which the CPD appears minimal. In contrast, the inversion of profile C-C' (Figure 10) shows a much more erratic CPD, fluctuating between ~8 km within the Okavango rift zone to greater than 20 km along the flanking faults. The

indistinguishable CPD depths on either side of the Okavango Rift Zone are attributable to areas with non-magnetized rock, while the deeper CPDs at the north and south ends of the profile are associated with the Roibok complex and Karoo flood basalts, respectively.

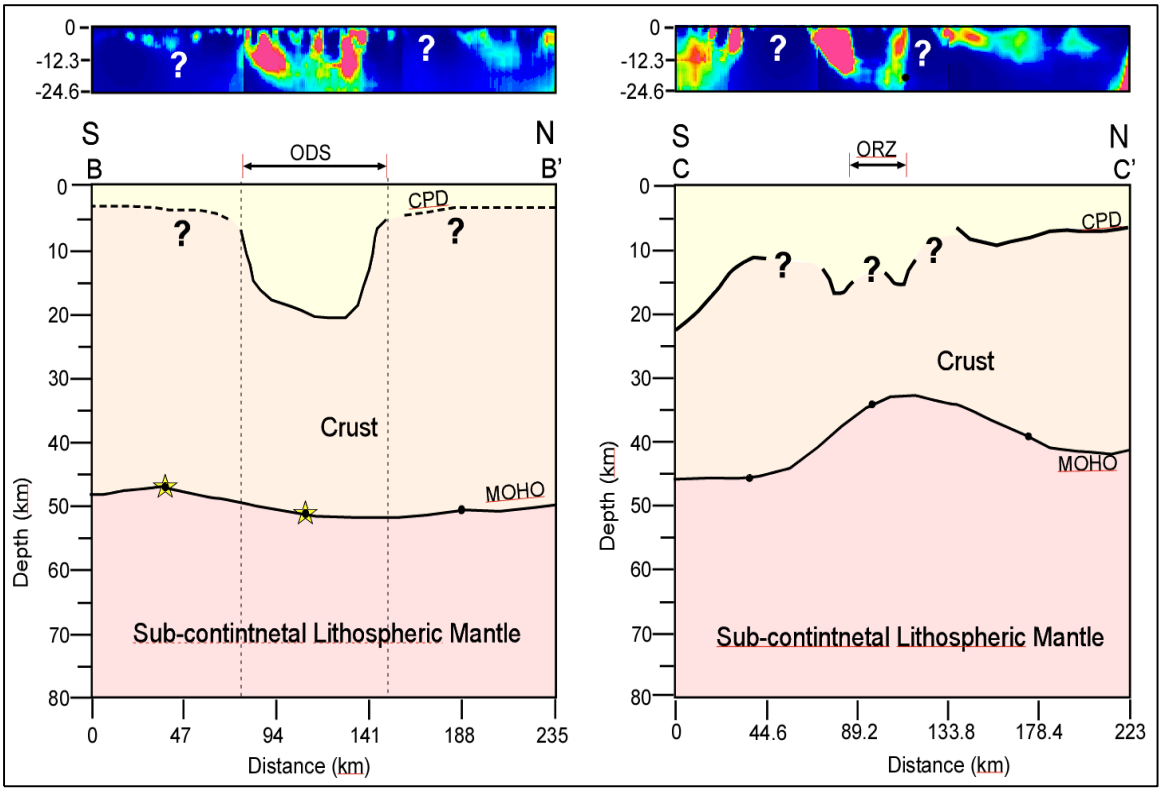

Figure 10: Schematic N-S sections (B-B', C-C' in Figure 5) illustrating the difference in lithospheric structure of the ODS within the Okavango Rift Zone and surrounding areas. The Moho under the ODS within the Okavango Rift Zone shallows to ~32 km. Away from the rift zone, the swarm is underlain by ~45 km continental crust similar to the surrounding Precambrian terranes. Additionally, away from the Okavango Rift Zone, the depth to the magnetized base is relatively deep under the ODS. Differently, the CPD under the rift zone suggests the superimposition of a shallower magnetic base on a deeper base forming a 'W—shaped" signature. Stars indicate passive seismic Moho estimates from Nair et al. (2006), Kgaswane et al. (2009), and Youssoff et al. (2013).

4.3 Crustal thickness variation under the Okavango dike swarm

The depth of the Mohorovičić discontinuity was calculated along the same profiles as the CPDs to create a crustal model below the ODS. The SE-NW profile A-A' (Figure 9) shows that the Moho gradually thins between the Kalahari suture zone and the Quangwadum complex with a minimum depth of 32 km below the incipient Okavango rift zone. This broad uplift spans a distance of 447 km. The Moho is thickest at the accretion zone of the Magondi orogenic belt and

Zimbabwe craton, with an estimated depth of 52 km (Figure 9). In the N-S profile B-B' (Figure 10), Moho depth estimates between 45-50 km below the swarm showed little variation from the surrounding terranes. In contrast, the Moho below the Okavango rift zone as shown in profile C-C' (Figure 10) is much shallower, occurring at a depth around 32 km. Additionally, the Moho is shallower to the north (~40 km) of the Okavango rift zone than to the south (~49 km).

CHAPTER V

DISCUSSION

Geological understanding of the emplacement of giant dike swarms such as the Mackenzie (>2000 km), the Gairdner (1000 km) and Okavango (~1500 km) remains limited, due in large part to a lack of exposure, but also due to oversimplification of dike propagation mechanics. A fundamental question arises; how can magma propagate for thousands of kilometers within cold inhomogeneous continental lithosphere? Results are discussed in light of existing models (failed rift arm and pre-existing structures) proposed for the ODS by previous authors (Reeves, 2000; Watkeys et al., 2002; Jourdan et al, 2004; Le Gall et al., 2005). Then an alternative model for the emplacement of the dike swarms is propose guided by our observations of the high-resolution geophysical data sets and supported by dike emplacement models produced through current observations within Afar and Iceland.

5.1 Palaeostress field and direction of fracture opening

In general, dike swarms exhibit trends parallel to the regional maximum compressive stress direction and perpendicular to the tensional stress direction (Pollard, 1987). However, new models proposed for the development of giant dike swarms are beginning to account for the contribution of preexisting discontinuities on the direction

and geometry of the dikes during emplacement (Le Gall et al., 2005; Hou et al., 2010; Ju et al., 2013). As such, it has been proposed, based on the difference in average dike widths between the N110°E ODS and N70°E SLDS, that the direction of extension during the Jurassic was oriented NNW-SSE (~ N160°E), wherein the ODS opened as oblique shear (sinistral) fracture system (Le Gall et al., 2005). On the regional scale, the basement fabric shows no signs of N110°E displacement, indicating that the shear sense observed from field observations is minor relative to normal tension (Figure 3). The direction of extension for northern Botswana during the Jurassic is considered herein to have been oriented ENE-WSW (≈N20°E). As such, it is proposed that the ODS opened primarily as a pure tensional fracture system, with a minor shearing component indicated by the presence of right and left stepping satellite dikes. The extensional stress direction proposed above is concordant with the icosahedral stress tessellations superimposed onto the restored Mesozoic configuration of Gondwana (Figure 4).

5.2 Was the emplacement of the Okavango Dike Swarm associated with rifting?

The ODS has been classically referred to as the failed third arm of a rifted triple junction (Figure 1; Burke & Dewey, 1973; Reeves, 1978; 2000). Regardless of whether or not a rift zone has failed or proceeded to continental breakup, these zones of lithospheric-scale weakness are characterized by a number of geophysically definable characteristics. These include: (1) an anomalous thin crust, hence an elevated Moho, (2) An elevated CPD (~10 km deep), (3) the presence of positive gravity anomaly that runs along the entire length of the rift system, and (4) the presence of border faults, grabens and half-grabens. In contrast to a number of younger (Rio Grande, Benue Trough, Muglad) and older (Olso, Midcontinent) rift systems throughout Africa

and North America (Chase and Gilmer, 1973; Benkhelil, 1989; Baldrige et al, 1991; Mohamed et al, 2001; Ebbing et al., 2007), the ODS lacks all or most of these common characteristics.

5.2.1. The lack of crustal thinning under the Okavango Dike Swarm

Many paleo-rifts exhibit classic features of the pure shear model of McKenzie, 1978 wherein the basin under extension undergoes brittle failure in the upper crust, resulting in faulting and graben formation, while the lower upper mantle deformed through ductile stretching, resulting in an overall isostatic subsidence of the ground surface and elevation of the Moho beneath the rift (Fairhead et al., 2013). By contrast, the addition of basaltic material to the lower crust (underplating) can contribute substantially towards thickening of the lithosphere and subsequently to the downward displacement of the Moho (Schmus and Hinze, 1985; Sundvoll and Larsen, 1993; Ziegler and Cloetingh, 2004).

Our lithospheric models below the ODS (Figures 9 and 10) show a maximum crustal thickness of ~52 km, with an average of 42±3 km. These thickness estimates from our gravity data are nearly identical (± 1 km) to published passive seismic values for the same areas (Table 1; Nair et al., 2006; Kgaswane et al., 2009; Youssoff et al., 2013), indicating that a window size of ~1°x1° was sufficient enough to resolve the crust- mantle boundary. Variation in depth to the Moho along strike (Figure 9) can be attributed to a thicker accretionary wedge at the boundary of the Zimbabwe craton and a developing thermal perturbation below the Okavango rift zone (Leseane et al., in review). Geophysical investigations of rift systems such as the Benue Trough (Adighije, 1981), Rio Grande rift (Olsen et al., 1987; Chapin 2013), Muglad basin (Fairhead et al., 2012) and the northern segment of the Rhine graben (Brun et al., 1992) have demonstrated the existence of a domed Moho under the rift axis, at depths ranging between 22 and 33 km. The persistent 45-50 km Moho depth measured under the ODS (Figure 10) suggests that the upper lithosphere has not been significantly disturbed, which consequently eliminates the probability that underplating exists below the ODS. Thus, the ODS was not emplaced in association with the development of a rift system.

5.2.2. The lack of elevated Curie Point Depths under the Okavango Dike Swarms

A recent MT study by Miensopust et al. (2011) depicted the ODS as a highly resistive body extending to a depth of ~60 km, indicating that our 3D inversion estimation of 25 km (Figure 9) are well within reason, given the same level of rheological and structural constraints. The discrepancy in depth between our inversions and the MT profile to the base of the swarm may be related to data smearing with depth, in an area bounded by deep, highly resistant cratons. In their discussion, Miensopust et al. (2011) stated that due to the relative thickness of the dikes, they should be treated as anisotropic at the MT scale and that the depth to the base of the ODS may not be reliable. Saleh et al. (2013) showed that the CPD is dependent upon geological conditions (heat flow and tectonic activity) and that depth to the bottom of the magnetized crust typically lies above the Moho, therefore representing a thermal rather than a compositional boundary. Given this, and provided the fact that the Moho extends to a depth of 42±3 km, based on passive seismic results, our estimation of the depth to the base of the highly magnetic ODS is acceptable, as larger inversion windows did not produce results below 25 km.

The discontinuous nature of the susceptibility at greater depths and relative continuity at lesser depths (Figure 9) imply that the dikes were emplaced within the upper 8-10 km of the current crust. This interpretation is supported by the field observations of Stansfield, (1975), who argued that the dikes themselves made-up only a fraction of the total thickness of the crust. Those who would argue that the magnetic data is ill-suited to resolving deep trends and that our interpretation is merely the shallowest possible CPD, must take into consideration the fact that the ODS is by far the most pronounced and well defined magnetic feature in northern Botswana. It is unlikely that a shallower magnetic layer would overshadow the ODS, especially following a moderate upward continuation. Numerous studies have shown that the shallowest CPDs (<15 km) are consistent with regions subjected to higher lithospheric temperatures, either due to magma intrusion or near surface hot springs (Mayhew, 1982; Maden, 2010; Hussein et al., 2013). Such is

not the case below the ODS. We interpret the deep semi-rounded high susceptibility anomalies along-strike of the ODS as fossilized mid-crustal feeder chambers, whose sizes and shapes were controlled in part by basement heterogeneities (folds and fractures associated with Proterozoic terranes). These chambers are approximately 15 km in diameter and extend toward the surface as narrow linear magnetic features, potentially representing groups of feeder dikes (Figure 8). Thus, our observations of the magnetic structure below the ODS are inconsistent with the common thermal structure below failed rift systems.

5.2.3. The lack of positive gravity anomaly along the Okavango Dike Swarms

Enhanced sedimentation in rift zones during surface subsidence typically generates a narrow negative Bouguer anomaly that is superimposed on a longer wavelength positive anomaly due to crustal thinning and in some cases the presence of a high density intrusive body at depth (Ebbing et al., 2007). Northern Botswana is dominated by linear NE-SW trending gravity anomalies (Figure 5; Yawsangratt, 2002). These gravity maxima are discordant with the WNW-trend of the ODS, and there does not appear to be a gravity minimum along the trace of the center of the swarm (Figure 5). Nevertheless, the lack of a gravity minimum signature along-strike may be attributable to peneplanation prior to deposition of the current Kalahari sedimentary cover. Based on the densities of major rock groups in Botswana and outcrop observations, it has been determined that the maximum anomaly values were caused by greenstone belts (Matsitama, Maitengwe, Vumba, and Tati) associated with the Achaean basement (Aldiss, 1991; Zeh et al., 1994; Majaule et al., 2001; Bagai et al., 2002; McCourt et al., 2004). In contrast with the Lebombo and Save-Limpopo dike swarms, the ODS lacks the presence of a persistent gravity high below its along-strike length, suggesting that it did not form as an aulacogen (Figures 1 and 5). It is possible that the absent gravity high is attributable to a poor density contrast between the doleritic dikes and Precambrian basement complex, but would fail to explain why the other two swarms are so prominent, if not because they are successful rift zones (Watkey et al., 2002). Despite similarities in Precambrian basement rheology between the central U.S. and southern

Africa, the pronounced gravity signature of the Mid-continental rift in contrast to the ODS, further advocates the absence of underplating within northern Botswana (Schmus and Hinze, 1985; Key and Ayres, 2000; Singletary et al., 2003).

5.2.4. The lack of brittle extensional structure along the Okavango Dike Swarms

Geologic observations and geophysical interpretations have shown that boundary faults are prominent features within incipient and paleo-rift systems (Ziegler and Cloetingh, 2004; Bufford et al., 2012). Our regional structural interpretation of northern Botswana from the aeromagnetic data does not show any WNW-trending structures aside from the ODS and satellite dikes (Figure 7). Given the sharpness of the edges of the ODS, one would expect to see the existence of a superimposed WNW-ESE brittle structural grain or a series of major faults aligned parallel to the swarm if they were formed in association with a rift system. As example, Figure 11 clearly shows the presence of border faults along the ORZ, while the region along the Shashe River, where the dikes are exposed (<50 m of sediment cover) shows no indications of faulting. The general absence of these features cannot be attributed to the resolution of the airborne geophysical datasets or the depth to the top of the buried basement rocks, as faults associated with the much narrower Okavango rift zone are clearly visible (Figures 7 and 11). Additionally, the depth to the top of the ODS, with exception to the area across the ORZ, is not more than 250 meters, which should not obscure imaging of normal faults if they were present, even those with minor displacements. As such, we propose that the absence of these distinctive structural features is another line of evidence against considering the swarm as an aulacogen-related dike intrusion, regardless of whether they were pre-, syn-, or post-rifting.

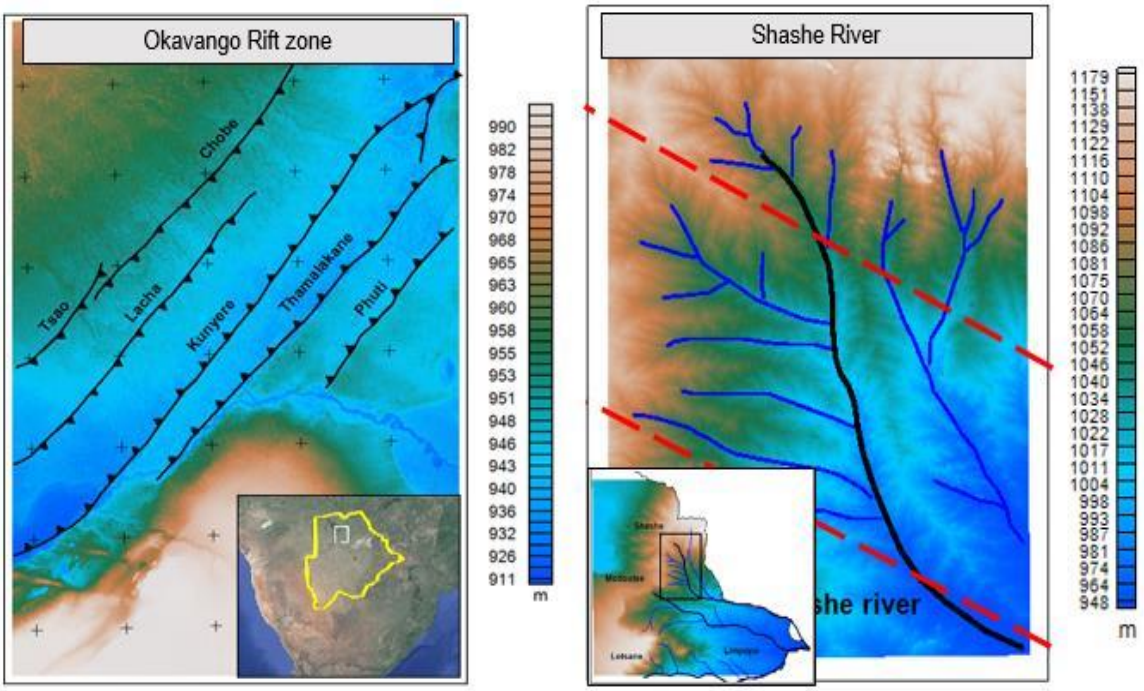

Figure 11: Satellite Radar Topography Mission (SRTM) digital elevation models over the incipient Okavango rift zone and Shashe river area, northern Botswana. Border faults are clearly visible along the axis of the ORZ, while they appear completely absent along the borders of the ODS, even in the region where they are known to outcrop at the surface. Red dashed line indicates edges of ODS.

5.3 Was the emplacement of the Okavango Dike Swarm guided by pre-existing structures?

Both the magnetic and gravity fabric (Figures 3 and 5) of the Proterozoic basement is predominantly ENE trending, while the ODS is WNW. The ODS crosses the width of Botswana without interruption or diminution, indicating that the mechanism by which the dikes were emplaced was acting so quickly and with such certainty that it had little time or interest in the preexisting grain of the basement rocks being penetrated. Within the last two decades, numerous studies involving geochemical (Duncan et. al., 1997; Elburg and Goldberg, 2000; Jourdan et al., 2004; Jourdan et al., 2007), structural (Le Gall et al., 2005), geochronological (Le Gall et al., 2002; Jourdan et al., 2006), and magnetic fabric (Aubourg et al., 2008) analyses have discredited the deep mantle plume origin for the Karoo Triple Junction. When observed with respect to a Jurassic reconstruction of Gondwana (Lawver et al. 1999), the Karoo Triple Junction is one of

many triple junctions across the supercontinent, which collectively form a tessellation network (Figure 4) following Euler's formula for the organization of plates on a spherical shell.

The distribution and arrangement of these fracture networks were self-organized based on the size and shape of Gondwana and the locations of pre-existing suture zones around its boundaries (Anderson, 1982; Sears et al. 2001; 2004). The 120° x 120° x 120° relationship between the Karoo dike swarms is consistent with columnar joint studies, which indicate that a crack will propagate to a critical length based on the thickness and strength of the medium before bending at 120° to resolve strain within the adjacent regions. Thereafter, the bend forms a re-entrant that concentrates stress and initiates new cracks which propagate either toward or away from the bend to create a triple junction (Budkewitsch and Robin, 1994; Jagla and Rojo, 2002). The branched cracks may then continue to propagate and bend until they form interconnected polygons and hexagons. It is suggested herein that the development of two arms of the Karoo triple junction fracture tessellation (Lebombo and Save-Limpopo; Figures 1 and 4) were influenced by pre-existing weak zones (Watkeys, 2002; Klausen, 2009), namely the ENE Limpopo orogenic belt, while the orientation of the ODS is merely coincidental, being partially influenced by Precambrian discontinuities, but largely controlled by the self-organization of the quasi-hexagonal fracture networks and associated stress distribution. Simply put, the ODS was emplaced within a lithospheric-scale crack, forced into the N110°E direction by the stabilization of the other triple junction arms.

Although the limited existence of WNW-trending dikes older than the ODS is irrefutable, their influence on the emplacement of the ODS and structural significance in the framework of southern Africa remains to be determined. It is conceivable that the pre-Jurassic dikes developed in response to the WNW-ESE accretion of mobile belts throughout the Proterozoic, as dikes tend to propagate parallel to the direction of maximum compression. However, the extent to which these Proterozoic dikes extend into northern Botswana and the magnitude of the tectonic event responsible for their emplacement is yet to be resolved. Moreover, unlike the Jurassic dikes,

which appear to follow a Gondwana-scale fracture tessellation network across southern Africa (Figure 4), the orientation and extent of the Proterozoic dikes was likely constrained to the area within and below the Zimbabwe craton, which was disrupted during the formation of the Limpopo mobile belt.

The distribution of macroscopic fractures and joints within exposed crystalline basement rocks has been used to imply the existence of shallow crustal discontinuities developed during the Precambrian that were reactivated and filled with magma during the Jurassic (Le Gall et al., 2005). As such, it is suggested that the ODS followed a coeval fracture network formed by the interconnection of along strike crustal discontinuities preferentially opening to the ENE-WSW (≈N20°E) due to dilation by fluid injection. In the absence of any large N110°E Precambrian structures and limited knowledge of the extent of the Proterozoic dikes, it is instead recommended that the ODS was initially influenced by the older dike system(s), but acted on its own for a majority of the distance emplaced.

5.4 A proposed model for the emplacement of the Okavango Dike Swarm

Given the absence of common rift features associated with the ODS and an uncertain influence of the preexisting lithospheric-scale structures, "under what mechanism could the ODS have been emplaced over 1500 km?" The main parameters controlling long distance lateral dike injection are pressure, volume of magma, and magnitude and orientation of the stress in the lithosphere (Rubin, 1995; Fialko and Rubin, 1999). In the case of the equivalent sized Mackenzie dike swarm in Canada, dike emplacement close to the source region is considered to be controlled by a hydraulic gradient developed through dynamic uplift of the crust (Ernst and Baragar, 1992; Ernst et al, 1995; Ernst et al., 2001), while emplacement further away from the source was controlled by the regional stress field and in part by the basement fabric (McHone et al., 2004; Hou et al., 2010).

The absence of older Karoo basalts along the strike of the swarm (Figure 2) infers dynamic uplift along a WNW-ESE axis (Reeves, 1978). The hydraulic gradient induced by dynamic uplift could be a plausible mechanism for emplacement of the ODS. The cause of the uplift along this specific trend may be the result of an increased thermal gradient along a lithospheric-scale weakness, driven by fracturing of the upper lithosphere (Anderson 1982; 2001; Sears et al 2001). Nonetheless, there still remains the problem of how magma could propagate over such a long distance before solidification. Lister and Kerr (1991) used theoretical models to suggest that dikes as thin as 10 m could propagate laterally for thousands of kilometers given ideal conditions such as the absence of crustal deformation. In addition, Rubin (1993) suggested that basaltic magma with a viscosity of 10^0 to 10^2 Pascals and an initial pressure of 10 MPa could propagate to infinity without solidification, provided it maintained a temperate gradient of -1 °C/m.

Although the dikes of the ODS meet the theoretical minimum width (~17 m on average; Le Gall et al., 2005), the swarm cross-cuts the dominant basement fabric, which does not provide ideal conditions for emplacement along such a long distance. Additionally, the temperature gradient of -1°C/m cannot possibly be sustained along the entire 1500 km length of the ODS, as it would equate to a distal temperate of over 1.5 million degrees Celsius ($\Delta T = 1.5x10^6$ °C). Most dike propagation models are based on numerical assumptions and oversimplified structural and rheological variations within the lithosphere, which do not reflect reality. The ODS exists within a thermally altered and heavily deformed geologic area, and thus could not be justifiably explained using these simplified models. Furthermore, in currently active rifting areas, where the crust is thin and hot, dikes measured in real-time through interferometric synthetic aperture radar (InSAR), earthquake monitoring stations, and field observations have been shown to propagate only tens of kilometers (Ayele et al., 2009; Hjartartdottir et al., 2012)., implying that dike

injection and propagation is not as simple as previously considered; A single, large, deep seated source feeding into a constructive basement fabric.

Investigations following the September 2005 diking episode in the Manda Harraro rift zone (Ethiopia) and Krafla diking episodes (Iceland) have shown that small, relatively shallow (7-10 km) feeder chambers existed along the central axes of the rift segments during dike emplacement (Grönvold et al. 2008; Ayele et al., 2009; Hjartardottir et al., 2012). These magma chambers were inferred and constrained from geodetic methods, seismicity, and field observations collected during and following the intrusion episodes. In their model, Ayele et al., 2009 depicted a large, deep chamber (primary source) feeding dikes laterally, perpendicular to the direction of maximum tension, actively destabilizing unconnected crustal magma reservoirs (secondary source) that were at or near their critical stress state. These volumetrically small magma reservoirs maintained enough driving pressure (the difference between the magma pressure and the tectonic stress at the dike tip) to influence dike emplacement length. Although the ODS, has herein been disregarded as a rift zone, the mechanisms for dike emplacement and chamber formation remain the same.

The ODS was emplaced along a lithospheric-scale zone of weakness that developed as part of the lithospheric fracturing along the geometrically defined pattern, composed of quasi-hexagonal tessellation vertices under the conditions of isometric, uniaxial tension as depicted in Figure 4. The propagation of the ODS was then facilitated over the 1500 km distance through the presence of a series of mid-crustal axial feeder chambers, represented schematically in Figure 12, similar to those found in continental spreading centers (Wright et al., 2012). The deep, semi-rounded, high magnetic susceptibility anomalies, imaged under the ODS (Figure 9) represent the solidified form of these feeder magma chambers. Our conceptual model for the emplacement and propagation of the ODS is consistent with observations from Ethiopia and Iceland, wherein one or more sub-crustal feeder centers can be involved during a single episode of dike injection and that extensional stresses controlled the orientation and propagation length of the dikes or fissures

(Ayele et al., 2009; Hjartardottir et al., 2012; Rubin and Pollard, 1988). In both spreading centers, it is observed that the lateral propagation of the dikes continues for up to 70 km from the feeder magma chamber, indicating a decrease of magma volume to support further propagation.

In the case of the ODS, it is possible that the deeper (~24 km) and larger (~12 km) sub-crustal feeder chambers had sufficient volumes of magma to permit longer dike propagation on the order of a few hundred kilometers. The four channels (labeled a-d in Figures 7 and 12) form the WNW pathways through which the magma propagated, likely developing in response to the weaker nature of the Proterozoic mobile belts and tensional stresses. Deviation of channel "d" (Figures 7 and 12) attests to the loss of fluid volume and pressure, causing the dikes to rotate into the dominant ENE-WSW orientation of the major geologic terranes. The axial magma chambers fed into the established channels. The geometry of the magma chambers is not well constrained, but they may have been influenced by the ENE trending boundaries of the Precambrian terranes based on an observed coincidence between their locations and the terrane boundaries (Figure 9). Details of the pathways that transported melt from the lower crust to the discrete feeder chambers in the mid-upper crust is unclear from the presented data, but are likely to have involved decompression melting from the asthenosphere, where partial melts migrated upwards in response to fracturing of the upper lithosphere. Alterations of the local stresses resulting from the propagation of dikes may have activated these feeder chambers or triggered the necessary mechanisms in the lithosphere to initiate their development (Buck et al., 2006). Relating the above model directly to the fragmentation of Gondwana and precursory development of the Karoo Triple Junction is plausible. Further studies are needed to evaluate the deeper lithospheric structure under the ODS.

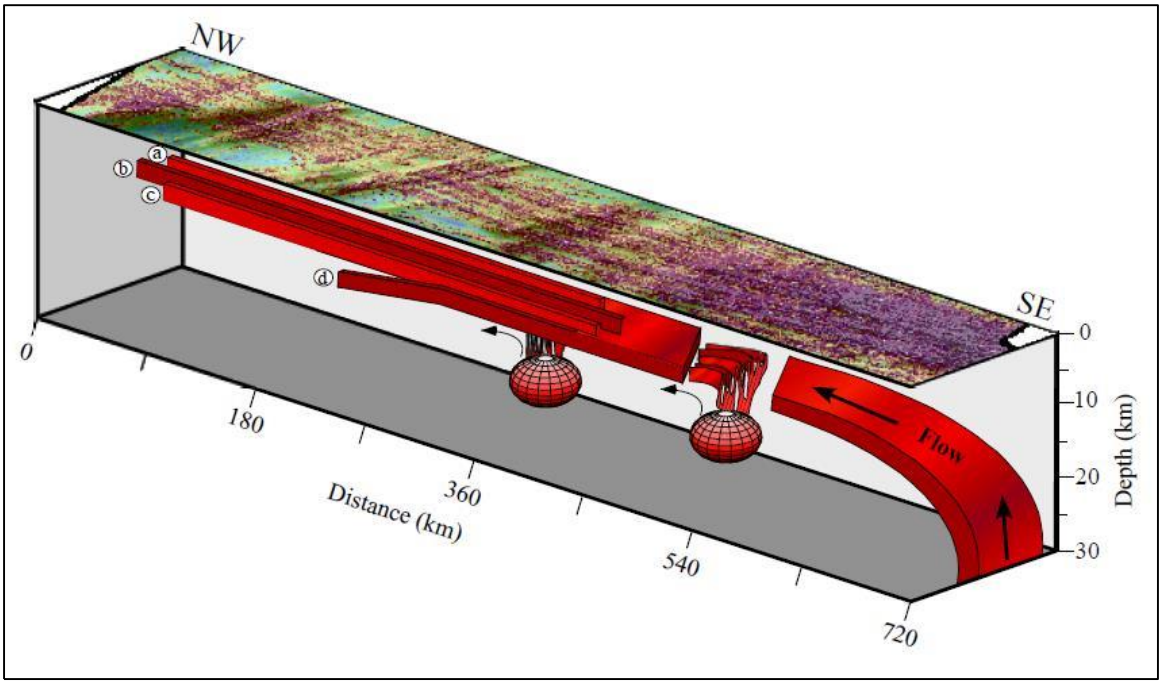

Figure 12: Dike emplacement model, showing division of the ODS into four channels (a-d). Within 300 km of the Mwenezi triple junction, the swarm was being fed vertically, but transitioned into dominantly lateral flow 400 km away from the triple junction. Magma chambers along-strike provided additional magma volume to allow for at least three of the four dike channels to propagate the 720 km across Botswana.

CHAPTER VI

CONCLUSIONS

Regional investigation of the ODS lithospheric structure using high-resolution aeromagnetic and gravity data in northern Botswana allowed us to evaluate the proposition that the swarm was emplaced in association with a failed arm of a rifted triple junction formed during the breakup of Gondwana, examine the possible role of pre-existing structure in shaping the orientation of the dike swarm, and propose an alternative emplacement model for the ODS. These are the major conclusions:

1. The lack of diagnostic characteristics of rift zones in the ODS (no anomalous thin crust, no elevated CPD, no linear positive gravity anomaly, no upper crust brittle deformation) led to the conclusion that the ODS did not develop in association with a failed rift or an aulacogen, despite its conspicuous geometrical arrangement as an arm of a rifted triple junction.
2. Geophysical results do not support any significant role for pre-existing structures in guiding the ODS to emplace for ~1500 km in a WNW-direction. However, there might be a minor role played by Proterozoic dike swarms of similar orientation in guiding the younger ODS. Additionally, we do not rule out the possibility of a similarly oriented deep lithospheric fracture formed during a Gondwana stagnation phase that followed its northward migration and preceded its dispersal.

3. The lack of a lateral displacement of the basement fabric along-strike of the ODS does not support the idea that the ODS opened purely as a sinistral shear fracture system. Instead, the ODS was emplaced primarily under pure tensile conditions, with a minor shearing component and a minimum stress axis oriented N20°E. The dikes followed a fracture tessellation network, controlled by Euler's formula for the organization of hexagonal plates on a spherical shell.
4. It is possible that the propagation of the ODS for over 1500 km distance was initiated by a hydraulic gradient associated with dynamic uplift along WNW-trending axis, partially influenced by the presence of Proterozoic dike swarms, and its emplacement along this length was maintained by a series of mid-crustal axial feeder chambers, whose location, size and shape were partially controlled by Precambrian basement structures. These fossilized chambers are 15 km in diameter and extend toward the surface as thin channels, potentially representing groups of feeder dikes. Details of the pathways that transported melt from the lower crust to the discrete feeder chambers in the mid-upper crust is likely to have involved decompression melting from the asthenosphere where partial melts migrated upwards in response to fracturing of the upper lithosphere.

REFERENCES

Adighije, C.I. (1981) A gravity interpretation of the Benue Trough, Nigeria, *Tectonophysics*, 79: 109-128.

Aldiss, D.T. (1991) The Motloutse Complex and the Zimbabwe Craton/Limpopo Belt transition in Botswana, *Precambrian Research*, 50: 1-2: 89-109.

Anderson, D.L. (1982) Hotspots, polar wander, Mesozoic convection and the Geoid. *Nature* 297:391-393.

Anderson, D.L. (1994) The sub-lithospheric mantle as the source of continental flood basalts; the case against the continental lithosphere and plume head reservoirs, *Earth and Planetary Science Letters* 123: 269- 280

Anderson, D.L. (2001) Top-down tectonics? *Science* 293: 2017-2018.

Anderson, D.L. (2002) Plate tectonics as a far-from-equilibrium self-organized system, in S. Stein and J. Freymuller, Eds. Plate Boundary Zones: AGU Monograph, Geodynamics Series 30, p. 411-425.

Aubourg, C., G. Tshoso, B. Le Gall, H. Bertrand, J.J. Tiercelin, A.B. Kampunzu, J. Dyment, M. Modisi (2008) Magma flow revealed by magnetic fabric in the Okavango giant dyke swarm, Karoo igneous province, northern Botswana, *Journal of Volcanology and Geothermal Research* 170: 247- 261.

Ayele, A., D. Keir, C. Ebinger, T.J. Wright, G.W. Stuart, W.R. Buck, E. Jacques, G. Ogubazghi, J. Sholan (2009) September 2005 mega-dike emplacement in the Manda-Harraro nascent oceanic rift (Afar depression), *Geophysical Research Letters*, 36: L20306, doi:10.1029/2009GL039605

Bagai, Z., R. Armstrong, A.B. Kampunzu (2002) U=Pb single zircon geochronology of granitoids in the Vumba granite-greenstone terrain (NE Botswana): Implications for the evolution of the Archean Zimbabwe Craton, *Precambrian Research* 118: 149-168

Baldridge, W.S., F.V. Perry, D.T. Vaniman, L.D. Nealey, B.D. Leavy, A.W. Laughlin, P. Kyle, Y. Bartov, G. Steinitz, E.S. Gladney (1991) Middle to late Cenozoic magmatism of the southeastern Colorado Plateau and central Rio Grande Rift (New Mexico and Arizona, U.S.A.): a model for continental rifting, *Tectonophysics*, 197: 327-354.

Benkhelil, J. (1989) The origin and evolution of the Cretaceous Benue Trough (Nigeria), *Journal of African Earth Sciences*, 8:2/3/4: 251-282.

Bordy, E.M., T. Segwabe, B. Makuke (2010) Sedimentology of the Upper Triassic-Lower Jurassic (?) Mosolotsane Formation (Karoo Supergroup), Kalahari Karoo Basin, Botswana, *Journal of African Earth Sciences* 58: 127-140.

Bouligand, C., J. Glen, R. Blakely (2009), Mapping Curie temperature depth in the western United States with a fractal model for crustal magnetization, *Journal of Geophysical Research* 114.

Brun, J.P., M.-A. Gutscher, DEKORP-ECORS teams (1992) Deep crustal structure of the Rhine Graben from DEKORP-ECORS seismic reflection data: a summary, *Tectonophysics* 208: 139-147.

Buck, W.R., P. Einarsson, B. Brandsdottir (2006) Tectonic stress and magma chamber size as controls on dike propagation: Constraints from the 1975-1984 Krafla rifting episode, *Journal of Geophysical Research* 111: B12404, doi:10.1029/2005JB003879

Budkewitsch, P., P.Y. Robin (1994) Modelling the evolution of columnar joint, *Journal of Geothermal Research*, 59: 219-239.

Bufford, K.M., Atekwana, E.A., Abdelsalam, M.G., Shemang, E., Atekwana, E.A., Mickus, K., Moidaki, M., Modisi, M.P., Molwalefhe, L. (2012) Geometry and faults tectonic activity 24 of the Okavango Rift Zone, Botswana: Evidence from magnetotelluric and electrical resistivity tomography imaging. *Journal of African Earth Sciences* 65, 61-71.

Burke, K., J.F. Dewey (1973) Plume generated triple junctions. Key indicators in applying plate tectonics to old rocks, *Journal of Geology* 81: 403-433.

Cambell, I.H. and Griffiths, R.W. (1990) Implications of the mantle plume structure for the evolution of flood basalts, *Earth and Planetary Letters* 90: 79-93.

Chase, C.G., T.H., Gilmer (1973) Precambrian plate tectonics: The midcontinent gravity high, *Earth and Planetary Science Letters*, 21 : 70-78.

Chapin, C. E. (2013) Evolution of the Rio Grande Rift – A Summary, in Rio Grande Rift: Tectonics and Magmatism (ed R. E. Riecker), American Geophysical Union, Washington, D. C.. doi: 10.1029/SP014p0001.

Courtillot, V., A. Davaille, J. Besse, J. Stock (2003) Three distinct types of hotspots in the Earth's mantle, *Earth and Planetary Science Letters* 205:295-308.

Cox, K.G, (1992) Karoo igneous activity, and the early stages of break-up of Gondwana, in *Magmatism and the Causes of Continental Breakup,* edited by B.C. Storey et al., *Geological Society London Special Publications* 68: 137-148.

Cruikshank, K.M., G. Zhao, A.M. Johnson (1991) Analysis of minor fractures associated with joints and faulted joints, *Journal of Structural Geology* 13:8:865-886.

Duncan, R.A., P.R. Hopper, J. Rehacek, J.S. Marsh, A.R. Duncan (1997) The timing and duration of the Karoo igneous event, southern Gondwana, *Journal of Geophyscial Research* 102:B8: 18,127 – 18,138.

Ebbing, J., J.R. Skilbrei, O. Olesen (2007) Insights into the magmatic architecture of the Oslo Graben by petrophyscially constrained analysis of the gravity and magnetic field, *Journal of Geophysical Research*, 112:B04404: 1-17

Elburg, M., A. Goldberg (2000) Age and geochemistry of Karoo dolerite dykes from northeast Botswana, *Jorunal of African Earth Sciences* 31:3/4: 539-554.

Ernst, R.E., and Baragar, W.R.A. (1992) Evidence from magnetic fabric for the flow pattern of magma in the Mackenzie giant radiating dyke swarm. *Nature* 356: 511-513.

Ernst, R.E., J.W. Head, E. Parfitt, E. Grosfils, L. Wilson (1995) Giant radiating dyke swarms on Earth and Venus, *Earth-Science Reviews* 39: 1-58.

Ernst, R.E., E.B. Grosfils, D. Mege (2001) Giant Dike Swarms: Earth, Venus, and Mars, *Annual Reviews. Earth Planet. Sci*. 29:489-534.

Fahrig, W.F., (1987) The tectonic setting of continental mafic dyke swarms: Failed arm and early passive margin, in Mafic Dyke Swarms, edited by H.C. Halls and W.F. Fahrig, *Geological Association of Canada Special Publication* 34: 331-348.

Fairhead, J.D., A. Salen, L. Cascone, M. Hammill, S. Masterton, E. Samson (2011) New Developments of the magnetic tilt-depth method to improve structural mapping of sedimentary basins, *Geophyscial Prospecting* 59:1072-1086.

Fairhead, J.D., C.M. Green, S.M. Masterton, R. Guiraud (2013) The role that plate tectonics, inferred stress changes and stratigraphic unconformities have on the evolution of the West and Central African Rift System and the Atlantic continental margins, 594: 118-127.

Fairhead, J.D., S. Mazur, C.M. Green, M.E. Yousif (2012) Regional tectonic controls on basement architecture and oil accumulation within the Muglad basin, Sudan, *ASES extended abstracts.*

Fialko, Y., A.M. Rubin (1999) Thermal and mechanical aspects of magma emplacement in giant dike swarms. *Journal of Geophysical Research* 104:23: 33-49

Fouch, M.J., D.E. James, J.C. VanDecar, S. van der Lee, Kaapvaal Seismic Group (2004) Mantle seismic structure beneath the Kaapvaal and Zimbabwe Cratons, *South African Journal of Geology* 107:33-44

Gomez, C.S, (2001) A catalogue of Dykes from Aeromagnetic surveys in Eastern and Southern Africa, *ITC Publication* 80

Gomez-Ortiz, D., R. Tejero- Lopez, R. Babin-Vich, A. Rivas-Ponce (2005) Crustal density structure in the Spanish Central System derived from gravity data analysis (Central Spain), *Tectonophysics*, 403:1-4: 131-149

Grönvold K, SA Halldórsson, G. Sigurðsson, G. Sverrisdóttir, N.Óskarsson (2008) Isotopic systematics of magma movement in the Krafla Central Volcano, North Iceland. In: Goldschmidt conference. Vancouver, Canada, p A331

Guiraud, R., Y. Bellion (1995) Late Carboniferous to recent geodynamic evolution of the west Gondwanian cratonic Tethyan margins. In: Nairn, A. Ricou, L.E., Vrielynck, B., Dercourt, J. (Eds.), The Ocean Basins and Margins 8, the Tethys Ocean. Plenum Press, New York, pp. 101-124.

Hamilton, W.B. (2003), An alternative Earth, *GSA Today* 13:11:4-12.

Hastie, W.W., M.K. Watkeys, C. Aubourg (2014) Magma flow in dyke swarms of the Karoo LIP: Implications for the mantle plume hypothesis, *Gondwana Reasearch*, http://dx.doi.org/10.1016/j.gr.2013.08.010.

Hjartardottir, A.R., P. Einarsson, E. Bramham, T. J. Wright (2012) The Krafla fissure swarm, Iceland, and its formation by rifting events, *Bulletin of Volcanology* 74: 2139-2153.

Hou, G., T.M. Kusky, C. Wang, Y. Wang (2010) Mechanics of the giant radiating Mackenzie dyke swarm: A paleostress field modeling, *Journal of Geophysical Research*, 115: B02402, doi:10.1029/2007JB005475

Hussein, M., K. Mickus, L.F. Serpa (2013) Curie Point Depth Estimates from Aeromagnetic Data from Death Valley and Surrounding Regions, California, *Pure and Applied Geophysics* 170:617-632.

Jagla, E.A., A.G. Rojo (2002) Sequential fragmentation: The origin of columnar quasihexagonal patterns, Physical Review E 65:026203.

Johnson, M.R, C.J. Van Vuuren, W.F. Hegenberger, R. Key, U. Shoko (1996) Stratigraphy of the Karoo Supergroup in southern Africa: an overview, *Journal of Africa Sciences* 23:1: 3-15.

Jones, C.R. (1980) The Geology of the Kalahari, *Botswana Notes and Records* 12: 1-14.

Jourdan, F., G. Feraud, H. Bertrand, A.B. Kampunzu, G. Tshoso, B. Le Gall, J.J. Tiercelin, P. Capiez (2004) The Karoo triple junction questioned: evidence from Jurassic and Proterozoic 40Ar/39Ar ages and geochemistry of the giant Okavango dyke swarm (Botswana), *Earth and Planetary Science Letters* 222: 989-1006.

Jourdan, F., G Feraud, H. Bertrand, M.K. Watkeys, A.B. Kampunzu, B. Le Gall (2006) Basement control on dyke distribution in Large Igneous Provinces: Case study of the Karoo triple junction, *Earth and Planetary Science Letters* 241: 307-322.

Jourdan, F., H. Bertrand, U. Scharer, J. Blichert-toft, G. Feraud, A.B. Kampunzu (2007) Major and Trace Element and Sr, Nd, Hf, and Pb, Isotopic Compositions of the Karoo Large Igneous Province, Botswana- Zimbabwe: Lithosphere vs Mantle Plume Contribution, *Journal of Petrology* 48:6: 1043-1077.

Key, M.K., N. Ayers (2000) The 1998 edition of the National Geological Map of Botswana, *Journal of African Earth Sciences* 30:3: 427-451.

Kgaswane, E.M., A.A. Nyblade, J. Julia, Paul H. G.M. Dirks, R.J. Durrheim, M.E. Pasyanos (2009) Shear wave velocity structure of the lower crust in southern Africa: Evidence for compositional heterogeneity within Achaean and Proterozoic terrains, *Journal of Geophyscial Research* 114, B12304, doi:10.1029/2008JB006217.

Klausen, M.B. (2009) The Lebombo monocline and associated feeder dyke swarm: diagnostic of a successful and highly volcanic rifted margin? *Tectonophysics*, 48: 42-62.

Lawver, L.A., L.M. Gahagan, I.W.D. Dalziel (1999) A tight fit- Early Mesozoic Gondwana, A plate reconstruction perspective, Memoirs of National Institute of Polar Research Special Issue, 53: 214-229.

Le Gall, B., G. Tshoso, F. Jourdan, G. Feraud, H. Bertrand, J.J. Tiercelin, A.B. Kampunzu, M.P. Modisi, J. Dyment, M. Maia (2002) 40Ar/39Ar geochronology and structural data from the giant Okavango and related mafic dyke swarms, Karoo igneous province, northern Botswana, *Earth and Planetary Science Letters* 202: 595-606.

Le Gall, B., G. Tshoso, J. Dyment, A.B. Kampunzu, F. Jourdan, G. Feraud, H. Bertrand, C. Aubourg, W. Vetel (2005) The Okavango giant mafic dyke swarm (NE Botswana): its structural significance within the Karoo Large Igneous province, *Journal of Structural Geology* 27: 2234-2255.

Leseane, K., E.A. Atekwana, K.L. Mickus, M.G. Abdelsalam, E.M. Shemang, E.A. Atekwana (2014) Thermal Perturbations Beneath the Incipient Okavango Rift Zone, Northwest Botswana, *Submitted for review in the Journal and Geophysical Research.*

Li, Y., D.W. Oldenburger (1996) 3D inversion of magnetic data, *Geophyscis* 61:394-408.

Lister, J.R., R.C. Kerr (1991) Fluid-mechanical models of crack propogation and their application to magma-transport in dykes, *Journal of Geophysical Research,* 96:10049-10077.

Maden, N. (2010) Curie-point Depth from Spectral Analysis of Magnetic Data in Erciyes Stratovolcano (Central Turkey), *Pure and Applied Geophyscis* 167:349-358.

Majaule, T., R.E. Hanson, R.M. Key, S.J. Singletary, M.W. Martin, S.A. Bowring (2001) The Magondi Belt in northeast Botswana: regional relations and new geochronological data from the Sua Pan area, *Journal of African Earth Sciences* 32:2: 257-267.

Maus, S., V.P. Dimri (1995) Potential field power spectrum inversion for scaling geology, *Journal of Geophysical Research* 100:12,605-12,616.

Mayhew, M.A. (1982) Application of satellite magnetic anomaly data to curie isotherm mapping, *Journal of Geophysical Research* 87: 4846-4854.

McCourt, S., A.B. Kampunzu, Z. Bagai, R.A. Armstrong (2004) The crustal architecture of Archaean terranes in Northeastern Botswana, 107: 147-158.

McHone, J.G., D.L. Anderson, Y.A. Fialko (2004) Giant Dikes: Patterns and Plate Tectonics, *Giant Dike Patters, Mantleplumes.org, http://www.mantleplumes.org/GiantDikePatterns.html*

McKenzie, D. (1978) Some remarks on the development of sedimentary basins, *Earth and Planetary Science Letters*, 40 : 25-32.

Miensopust, M.P., A.G. Jones, M.R. Muller, X. Garcia, R.L. Evans (2011) Lithospheric structures and Precambrian terrane boundaries in northeastern Botswana revealed through magnetotelluric profiling as part of Southern African Magnetotelluric Experiment, *Journal of Geophysical Research*, 116: B02401: 1-21.

Modie, B.N.J. (1996) Depositional environments of Meso- to Neoproterozoic Ghanzi-Chobe belt, northwest Botswana, *Journal of African Earth Sciences* 22:3: 255-268.

Mohamed, A.Y., W.A. Ashcroft, A.J. Whiteman (2001) Structural development and crustal stretching in the Muglad basin, southern Sudan, *Journal of African Earth Sciences*, 32: 2: 179-191.

Morgan, W.J. (1981) Hotspot tracks and the opening of the Atlantic and Indian oceans, in *The Sea vol. 7,* edited by C. Emiliani: 433-475, Wiley Interscience, New York.

Nair, S.K., S.S. Gao, K.H. Liu, P.G. Silver (2006) Southern African crustal evolution and composition: Constraints from receiver function studies, *Journal of Geophyscial Research* 111: B02304, doi:10.1029/2005JB003802.

Olsen K.H., W.S. Baldridge, J.F. Callender (1987) Rio Grande rift: an overview, *Tectonophysics*, 143: 119-139.

Parker, A.J., Rickwood, P.C., Baillie, P.W., McClenaghan, M.P., Boyd, D.M., Freeman, M.J., Pietsch, B.A., Murray, C.G., and Myers, J.S. (1987) Mafic Dyke swarms of Australia. In H.C. Halls and W.F. Fahrig (Editors), Mafic Dyke Swarms. *Geol. Assoc. Can. Spec. Pap.* 34:401-417.

Pollard, D.D., (1987) Elementary fracture mechanics applied to the structured interpretation of dykes. In H.C. Halls and W.F. Fahrig, eds., Mafic Dyke Swarms. Special Paper 34 of the Geological Association of Canada, p. 5-24.

Reeves, C.V. (1978) A failed Gondwana spreading axis in southern Africa, *Nature* 273: 222-223.

Reeves, C.V. (2000) The geophysical mapping of Mesozoic dyke swarms in southern Africa and their origin in the disruption of Gondwana, *Journal of African Earth Sciences* 30: 499-513.

Rubin, A.M., **(1993)**, On the thermal viability of dikes leaving magma chambers: *Geophysical Research Letters.,* 20: 257-260.

Rubin, M.A. (1995) Propagation of magma-filled cracks, *Ann. Rev. Earth Planet. Sci.* 23: 287-336.

Rubin, M.A., D.D. Pollard (1988) Dike induced faulting in rift zones of Iceland and Afar, *Geology* 16:413-417.

Saleh, S., M. Salk, O. Pamukcu (2013) Estimating curie point depth and heat flow map for northern Red Sea Rift of Egypt and its surroundings, from aeromagnetic data, *Pure and applied geophysics* 170: 863-885.

Schmus W.R.C., W.J. Hinze (1985) The midcontinent rift system, *Annual Review of Earth and Planetary Sciences*, 13: 345-383.

Sears, J.W. (2001) Icosahedral fracture tessellation of early Mesoproterozoic Laurentia, *Geology* 29:4:327-330.

Sears, J.W., G.M. St. George, J.C. Winne (2004) Continental rift systems and anorogenic magmatism, *Lithos* 80:1-4:147-154.

Spector, A. and F. Grant (1970), Statistical models for interpreting aeromagnetic data, 750 *Geophysics* 35, 293–302.

Singletary, S.J., R.E. Hanson, M.W. Martin, J.L. Crowley, S.A. Bowring, R.M. Key, L.V. Ramokate, B.B. Direng, M.A. Krol (2003) Geochronology of basement rocks in the Kalahari Desert, Botswana, and implications for regional Proterozoic tectonics, *Precambrian Research* 121:47-71.

Stansfield, G. *The Geology of the Area around Dukwe and Tlalamabele, Central District, Botswana*. Gaberone: Geological Survey Dept., Ministry of Mineral Resources and Water Affairs, Republic of Botswana, 1973.

Sundvoll, B., B.T, Larsen (1994) Architecture and early evolution of the Oslo Rift, *Tectonophysics* 240: 173-189.

Tselentis G. A., J. Drakopoulos and K. Dimtriads (1988), A spectral approach to moho depths estimation from gravity measurement in Epirus (NW Greece), *Journal of Physical Earth*, 36: 255-266.

Treloar, P.J. (1988) The geological evolution of the Magondi mobile belt, Zimbabwe, *Precambrian Research* 38:55-73.

Watkeys, M.K., (2002) Development of the Lebombo rifted volcanic margin of southeast Africa, in M.A. Menzies, S.L. Klemperer, C.J. Ebinger, J. Bake (Eds), Volcanic Rifted Margin, *Geological Society of America Special Paper*, 362: 29-48.

White, R., D. McKenzie (1989) Magmatism at rift zones: The generation of volcanic continental margins and flood basalts. *Journal of Geophysical Research* 94 :(B6): 7685-7729.

Wright, T.J., F. Sigmundsson, C. Pagli, M. Belachew, I.J. Hamling, B. Bradsdottir, D. Keir, R. Pedersen, A. Ayele, C. Ebinger, P. Einarsson, E. Lewi, E. Calais (2012) Geophysical constraints on the dynamics of spreading centers from the rifting episodes on land, *Nature Geoscience* 5:242-250.

Yawsangratt, S. (2002) A gravity study of Northern Botswana: a new perspective and its implications for regional geology. Enschede, ITC, 2002.

Youssof, M., H. Thybo, I.M. Artemieva, A. Levander (2013) Moho depth and crustal composition in Southern Africa, *Tectonophysics,* 609: 267-287.

Zeh, A., A. Gerdes, J.M. Barton (2009) Achaean Accretion and Crustal Evolution of the Kalahari Craton- the Zircon Age and Hf Isotope Record of Granitic Rocks from Barberton/Swaziland to Francistown Arc, *Journal of Petrology* 50:5:933-966.

Ziegler, P.A., S. Cloetingh (2004) Dynamic processes controlling evolution of rifted basins, *Earth-Science Reviews*, 64: 1-50.

APPENDICES

Appendix A: Other Applied Methods

I. Dip of the dikes

Dip of the buried dikes was evaluated using a visualization technique developed by Lahti and Karinin (2010), which combines the tilt derivative (TDR) technique of Miller and Singh (1994) with the procedure for multi-scale upward continuation introduced by Hornby et al., (1999), herein referred to as the TDR multi-scale edge technique. Unlike conventional derivatives (VDR, THDR, AS), the derivative ratio makes the tilt function independent of the amplitude of the total magnetic intensity (TMI) field and the susceptibility of causative bodies, both of which can be significantly influenced by remnant magnetization (Fairhead et al., 2011). The magnetic tilt angle is defined as

$$= \arctan\left[\frac{\partial M}{\partial h}\right]_M \quad (1)$$

Where $\frac{\partial M}{h} = \sqrt{\left(\frac{\partial M}{\partial}\right)^2 + \left(\frac{\partial M}{\partial}\right)^2}$

and $\frac{\partial M}{\partial}, \frac{M}{\partial}, \frac{M}{\partial}$

are first-order derivative of the magnetic field (M) in the x, y and z directions. Due to the nature of the arctangent function, all tilt angles are restricted to values between ±90°, regardless of the amplitudes of the individual derivatives (Salem et al., 2007; Miller and Singh, 1994). This constraint makes calculating the tilt angle similar to an automatic gain control (AGC) filter in that, it equalizes the amplitude output of magnetic anomalies across a profile or grid, so that both deep and shallow structures can be resolved (Verduzco et al., 2004). This method benefits from being less sensitive to noise in the data, which often increases with higher order derivatives. The dip of a body can be determined based on the asymmetry of the zero degree contour intervals

with varying upward continuation levels on a RTP-TDR filtered grid. The processing procedure is summarized in the flowchart below.

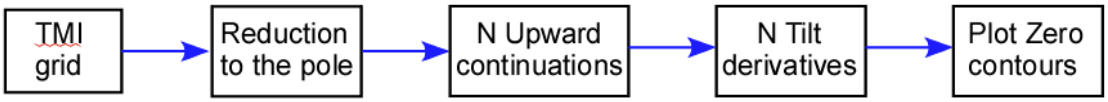

II. Depth to top of the swarm

Depth to the top of the swarm was determined using the *Tilt-depth* method developed by Salem et al., (2007; 2010), who used the assumptions: 1) contacts are nearly vertical, 2) the magnetic inclination is 90° (RTP) and 3) the anomalies are two-dimensional, to relate tilt angle with horizontal location (h) and source depth (z_c). As a result, the expressions for the vertical and horizontal derivatives of the TMI field over a contact were simplified such that when they were substituted back into equation 1 above, the inclination, declination, susceptibility contrast, and magnitude of the TMI field were eliminated, leaving

$$= \arctan\left[\frac{h}{z_c}\right] \qquad (2)$$

Where, h is the horizontal location of the anomaly and z_c is the source depth. Equation 2 indicates that the value of the tilt angle above the edge of the contacts is 0° at the position h=0 and equal to ± 45° at a horizontal position from the edges equal to the source depth (Salem et al., 2007). Depth to the causative anomaly can be calculated directly as half the physical distance between the ±45° tilt angle contours on the filtered TMI grid. A major advantage of this method over Euler deconvolution is that it does not require a user defined window size or pre-defined structural index (SI). Similarly, this method does not generate clouds of solutions because the depth estimates are anomaly-specific and typically conservative (Farihead et al., 2011). Breakdown of the 2-D assumption is depicted on the grid as a variation in the distance between the ±45° contours and the 0° contour around the perimeter of each body, which under ideal conditions would be symmetrical. This inconsistency was accounted for by breaking the swarm into twenty-five small rectangles, wherein 30 measurements were taken in each to determine a range and average across the sampled parts of the swarm. A profile of the swarm was created by subtracting the interpreted depth values from the SRTM along the same line.

Appendix B: Additional Methods Results

I. TDR multi-scale edge technique

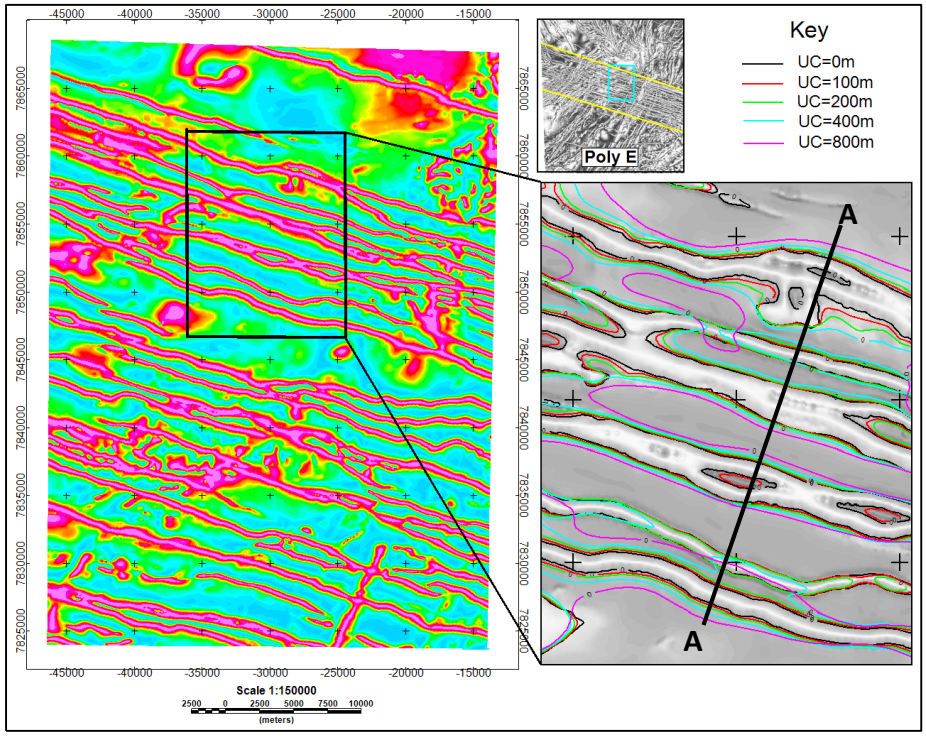

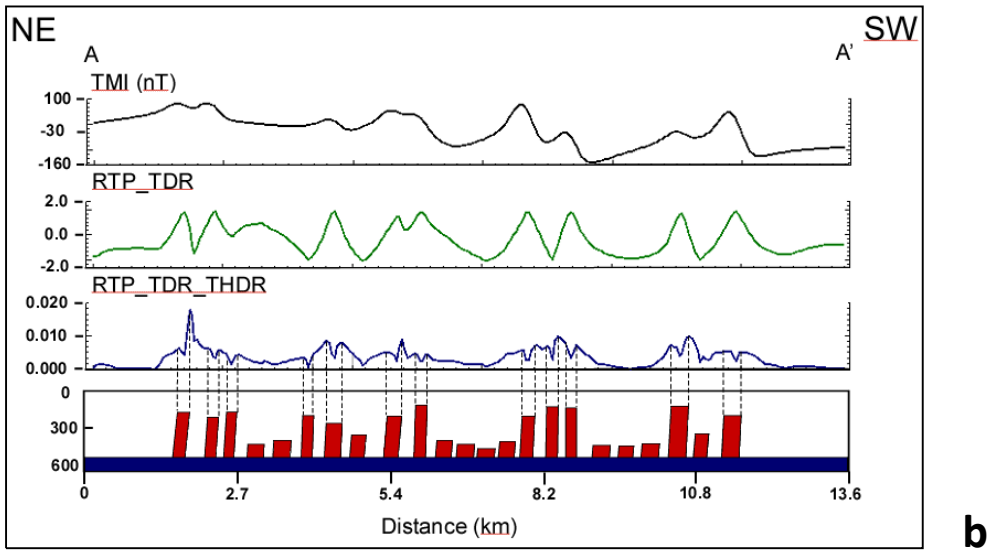

Fig 1. (a) Tilt-Derivative zero contour map of a 15x12km section of the ODS within polygon E (Fig 2), at the NW extent of the swarm in Botswana. Four upward continuation levels were applied. Grey-scaled background is the Reduced to Pole (RTP) corrected, low altitude airborne TMI grid. Data acquired from the Geological Survey of Botswana. (b) Interpretation of profile A-A' (shown in figure 3a) intersecting the NNW-SSE trend of eight TMI maximums, assumed to represent "dike families". Dashed lines identify approximate edges of shallower dikes.

II. Tilt-depth technique

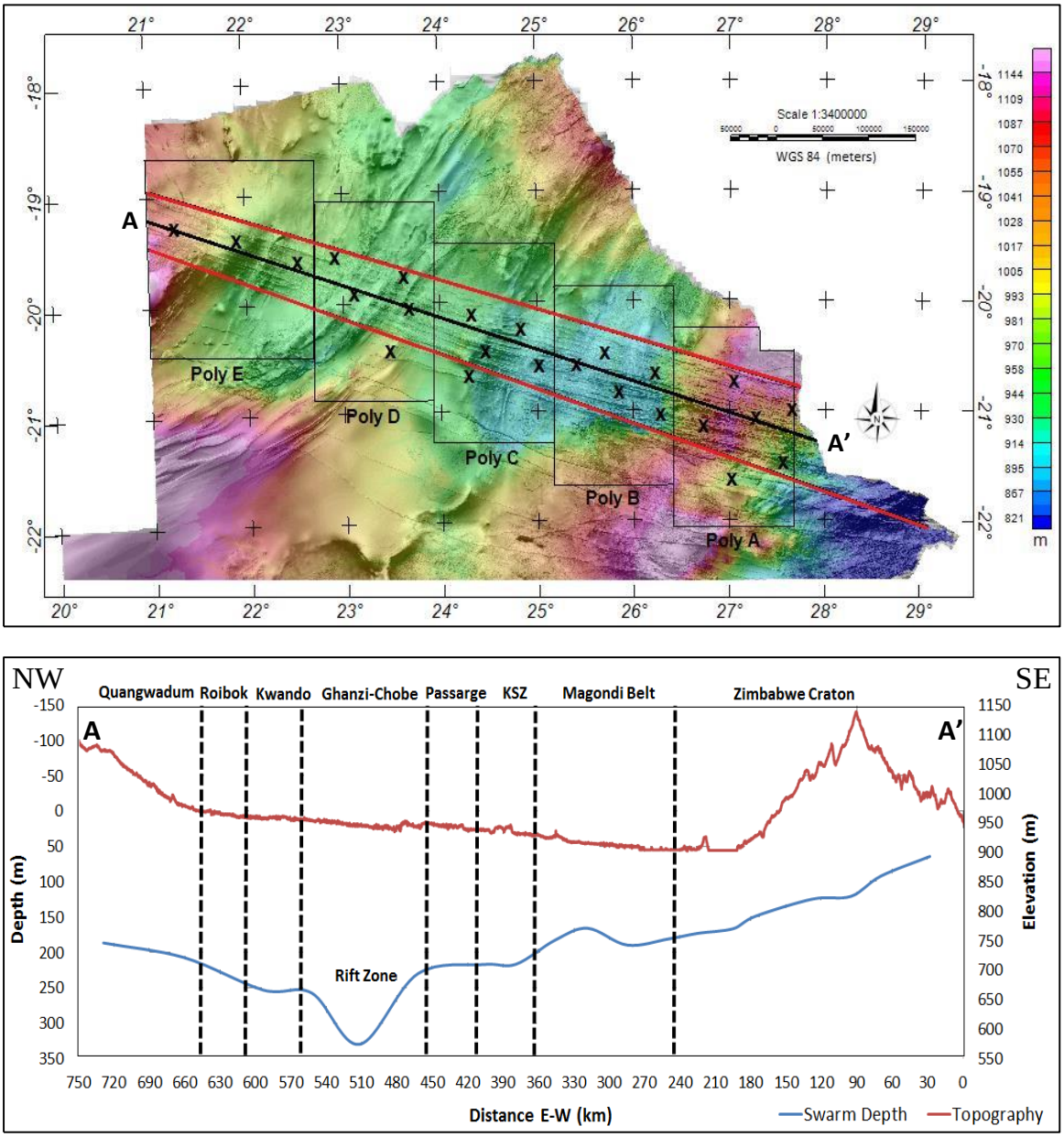

Fig 2. (a) Shuttle Radar Topography Mission (SRTM) Digital Elevation Model (DEM) of northern Botswana (90m spatial resolution). The swarm was subdivided in five zones (A-E) to improve resolution of individual dikes and reduce the influence of surrounding structures. Black X's represent the sample locations for the tilt depth technique developed by Salem et al., (2007; 2010) and red lines show the extent of the ODS. (b) Interpretation of profile A-A' (shown in figure a) along-strike the ODS, comparing the current topography (red/top curve) to the estimated depth to the top of the swarm (blue/bottom curve). Curves were plotted on separate Y-axis to prevent stretching, due to different scales.

Appendix C: Inversion Blocks

I. Selected Detailed Blocks

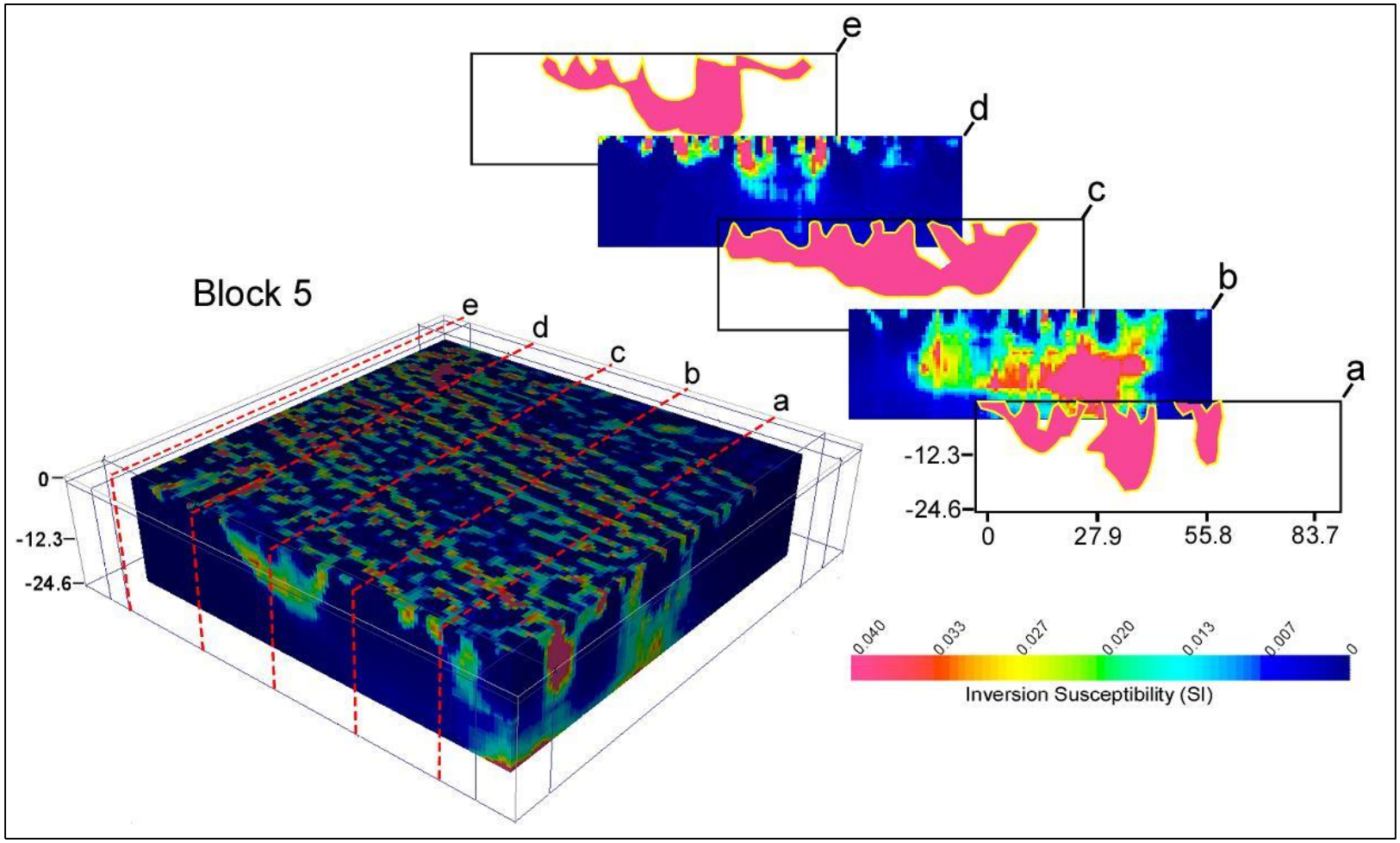

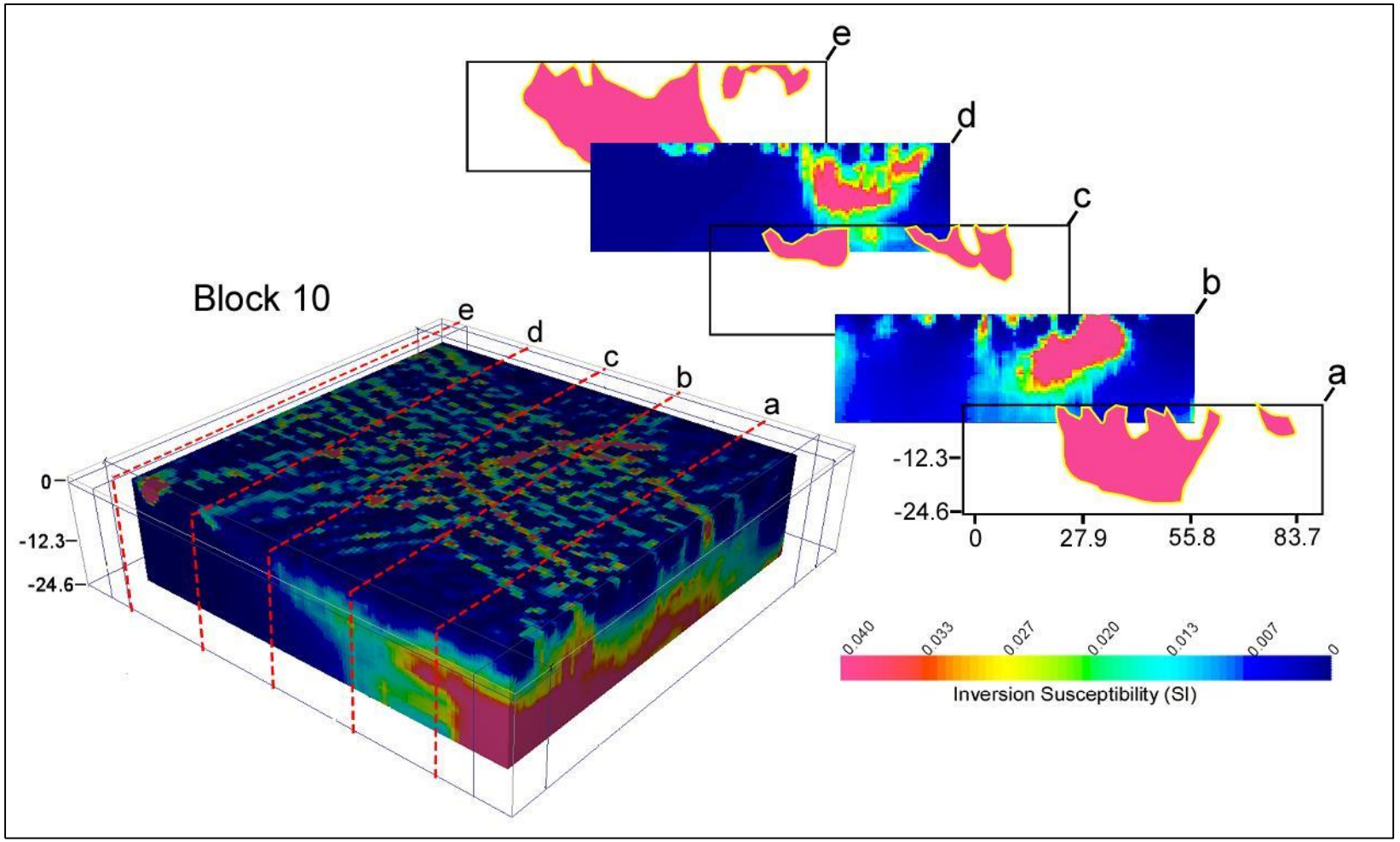
Block 10
e
d
c
b
a
0
-12.3
-24.6
0
27.9
55.8
83.7
0.040
0.033
0.027
0.020
0.013
0.007
0
Inversion Susceptibility (SI)

II. Additional Inversion Blocks

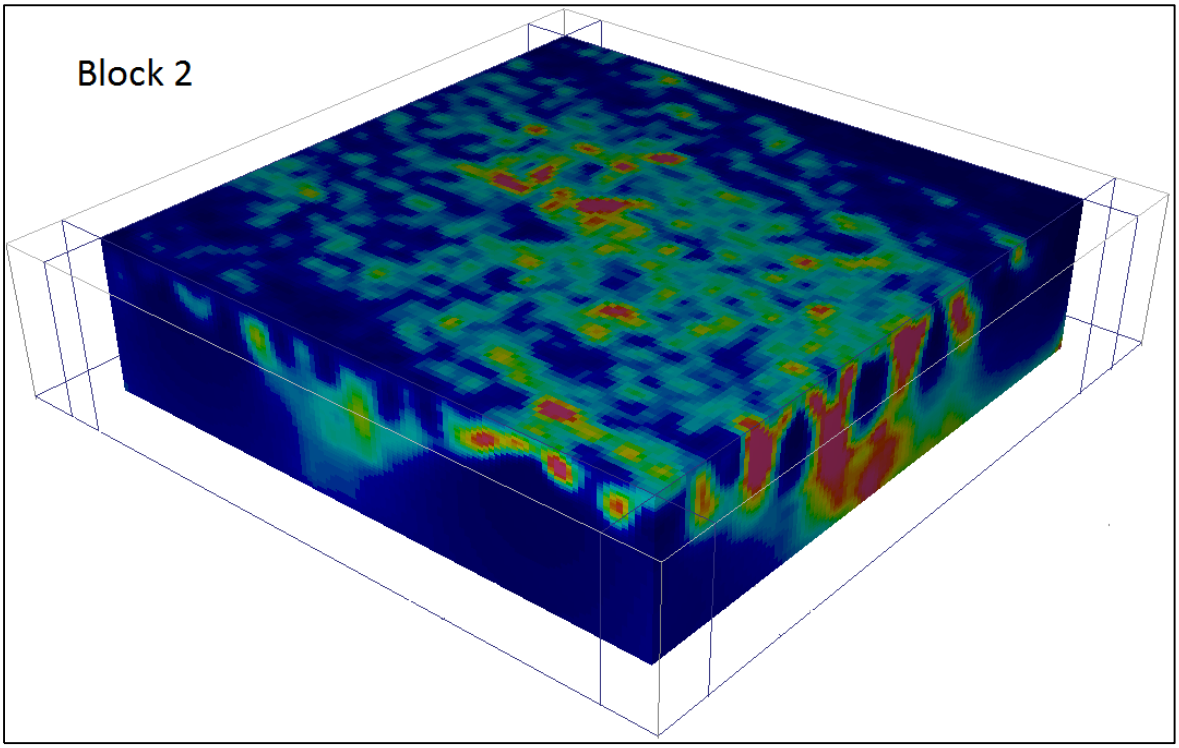

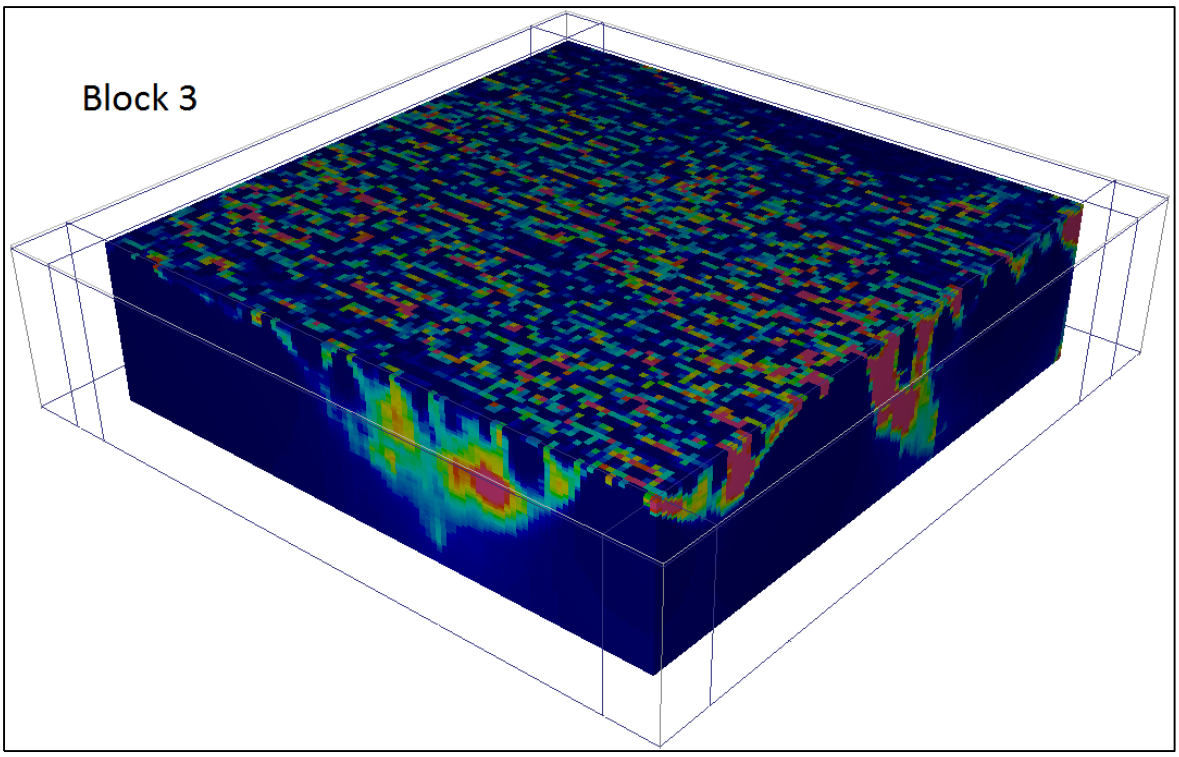

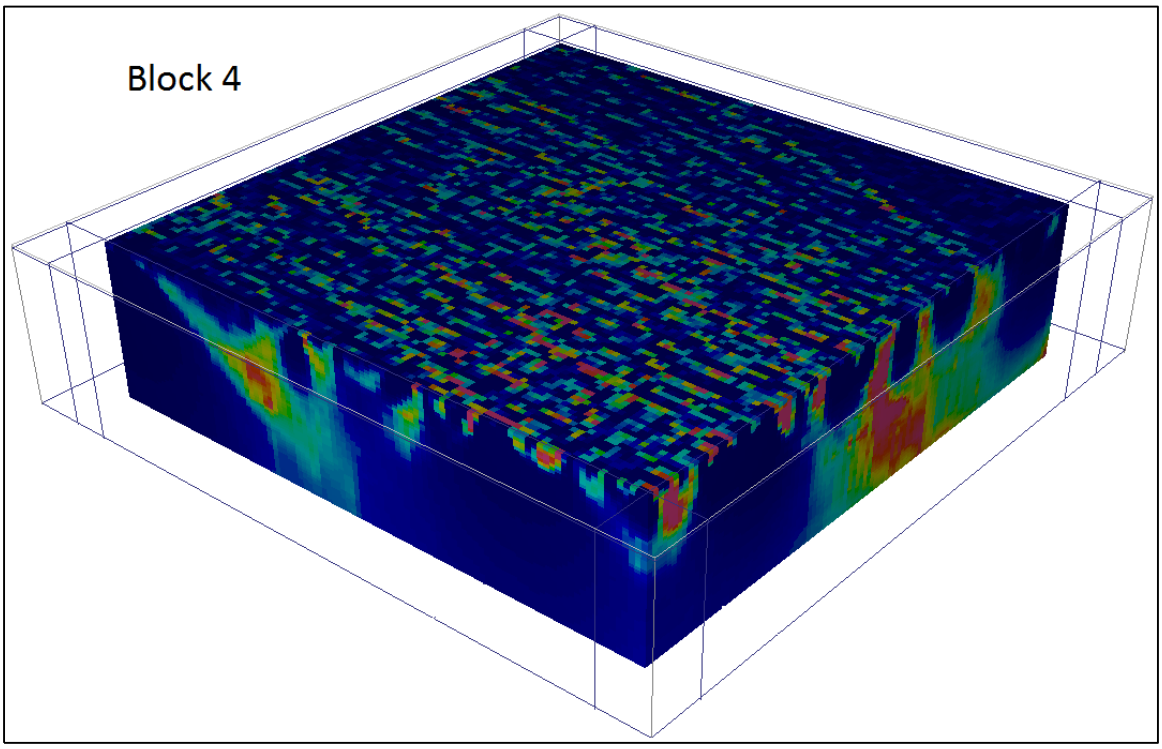
Block 4

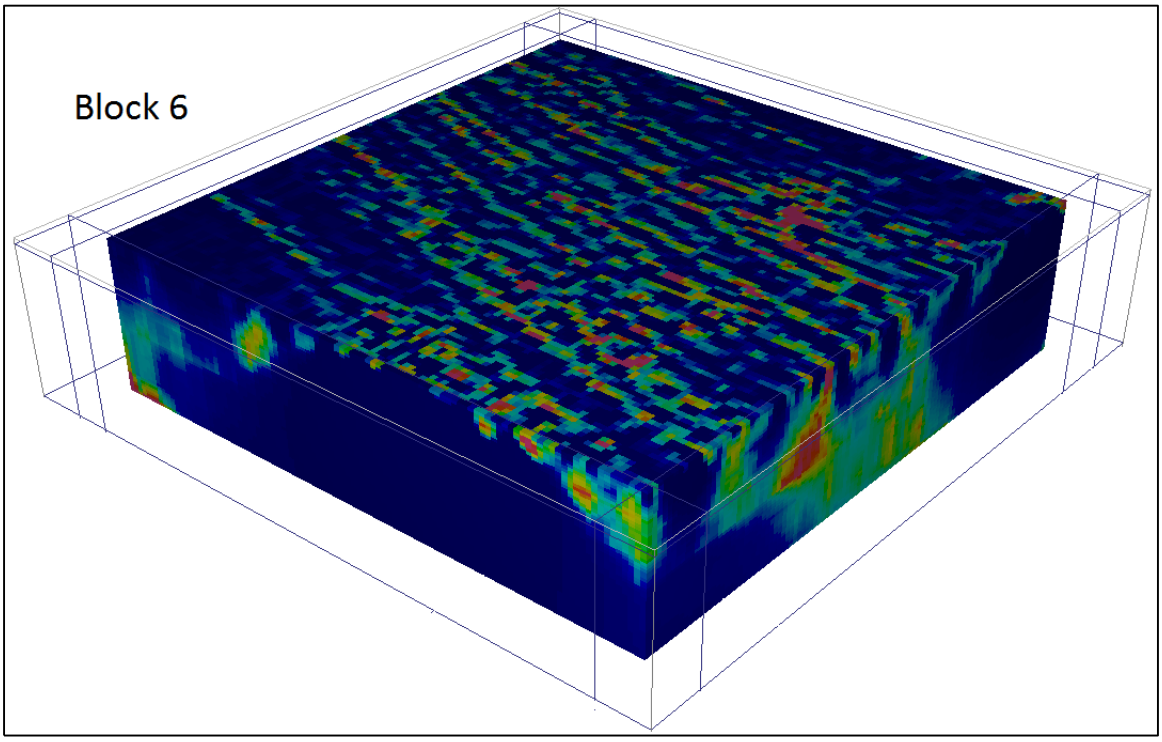
Block 6

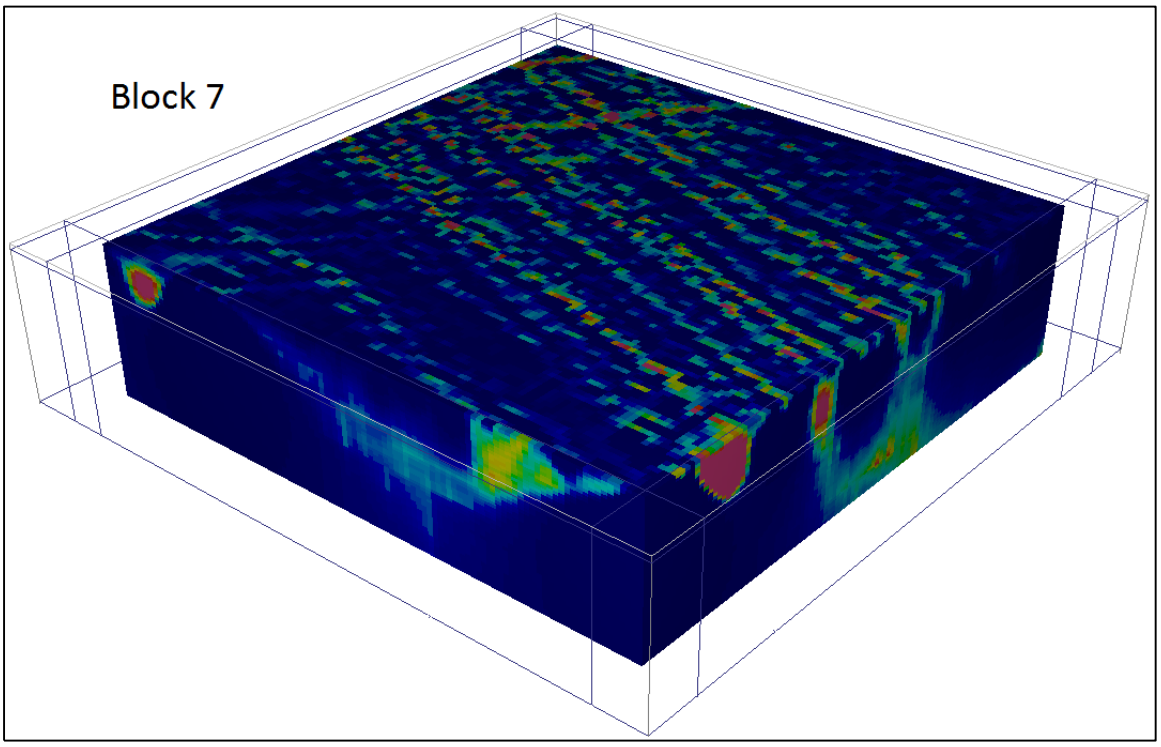
Block 7

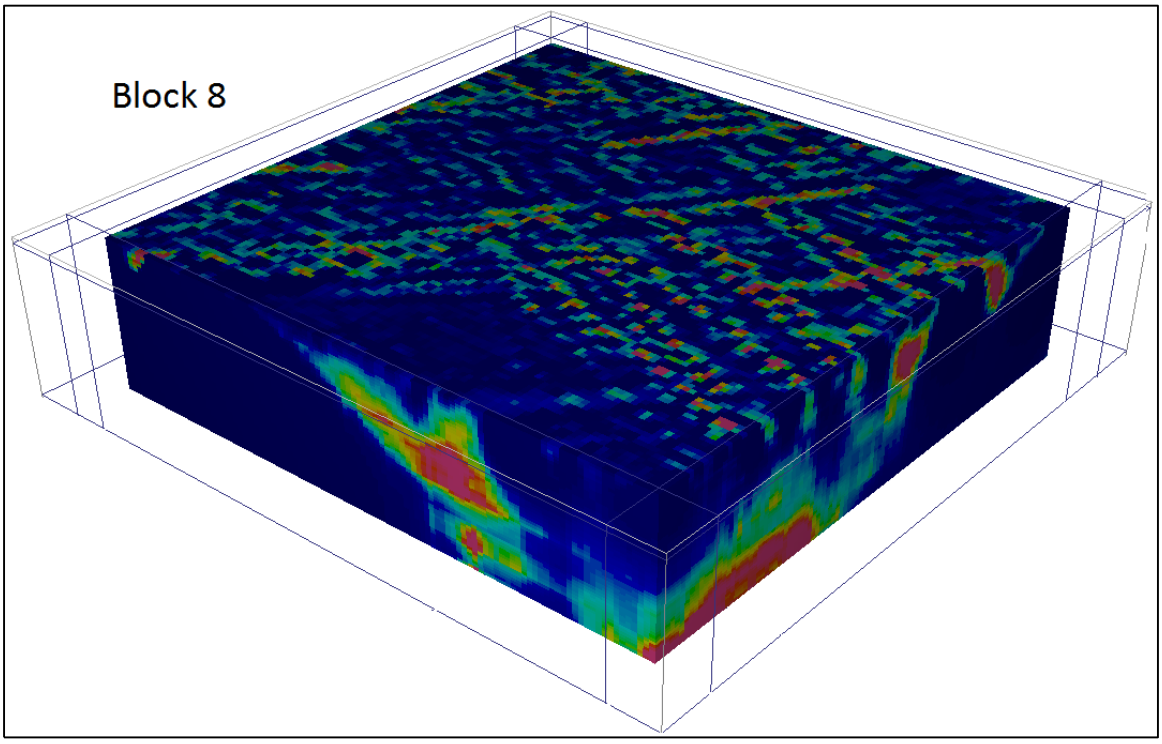
Block 8

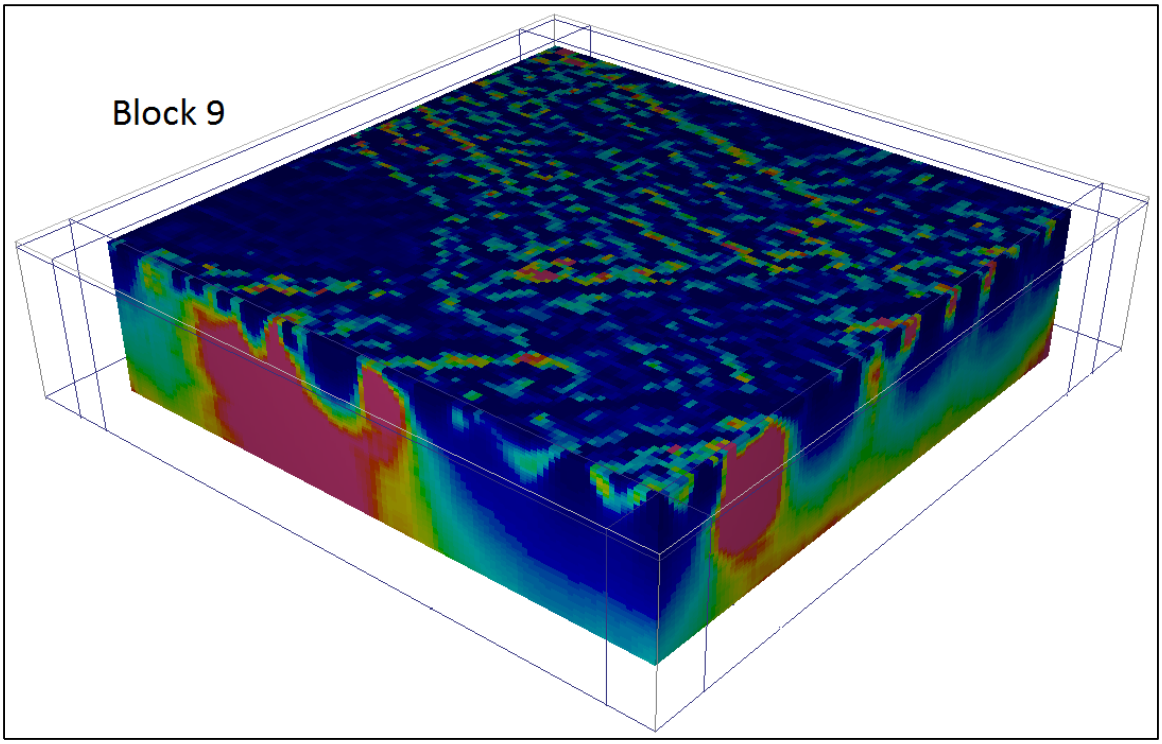
Block 9

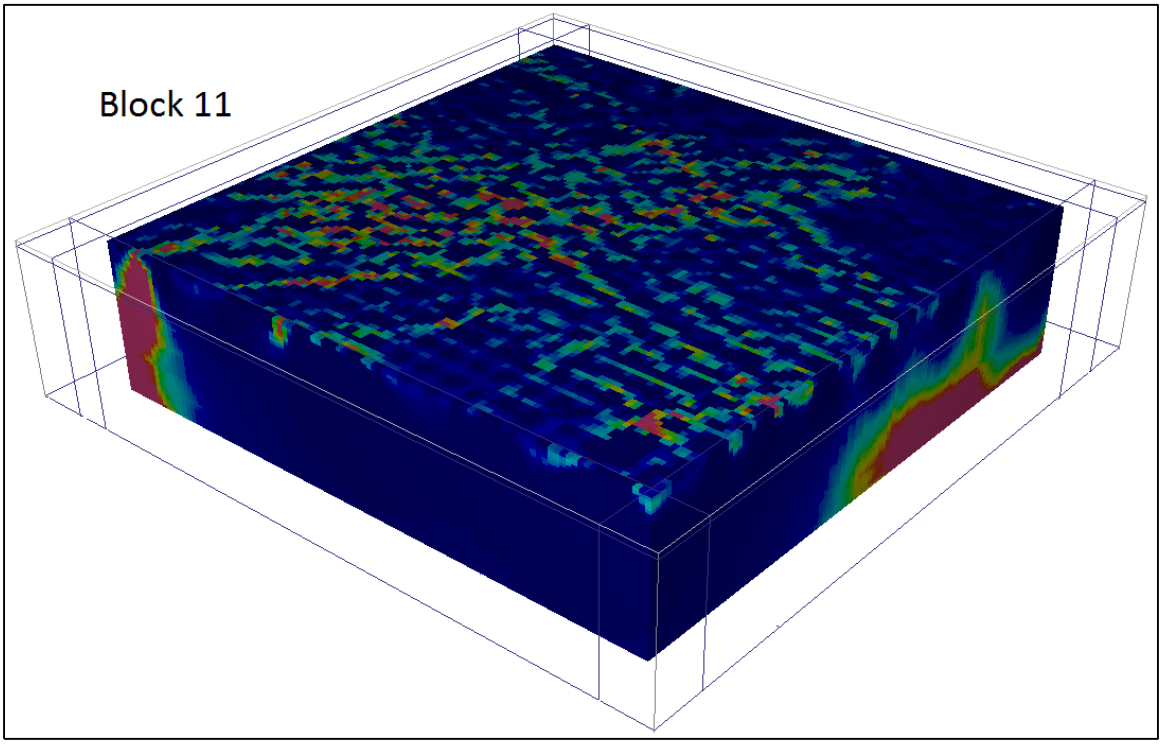
Block 11

VITA

Alan Keith Le Pera

Candidate for the Degree of

Master of Science

Thesis: STRUCTURE AND EMPLACEMENT OF THE GIANT OKAVANGO DIKE SWARM IN NORTHERN BOTSWANA: A NEW PERSPECTIVE FROM AIRBORNE GEOPHYSICAL DATA

Major Field: Geology

Biographical:

Education:

- Completed the requirements for the Master of Scienc in your Geology at Oklahoma State University, Stillwater, Oklahoma in May, 2014.

- Completed the requirements for the Bachelor of Science in your Environmental Geology at Rutgers University, Newark, NJ in 2012.

Experience:

- Geophysics Intern- Processed and interpreted 3D seismic data to high grade prospective formations; Summer 2013; Devon Energy, Oklahoma City, OK

- Research Assistant- NJWRRI grant funded laboratory and field data acquisition and analysis; Spring 2012- Summer 2012; Rutgers University, Newark NJ

- National Science Foundation Research - International research in Botswana; Summer 2011; Oklahoma State University, Stillwater, OK

Professional Memberships:

- Tulsa Geological Society, American Association of Petroleum Geologists, Society of Exploration Geophysicists, OSU Geological Society